Hydrothermal Synthesis and Characterization of Transition Metal Oxides

By

Aytaç ŞAHİN

**A Dissertation Submitted to the
Graduate School in Partial Fulfillment of the
Requirements for the Degree of**

MASTER OF SCIENCE

**Department: Materials Science and Engineering
Major: Materials Science**

**İzmir Institute of Technology
İzmir, Turkey**

October, 2004

We approve the thesis of **Aytaç ŞAHİN**

Date of Signature

---------- 22.10.2004

Assist.Prof.Dr. Mehtap EANES
Supervisor
Department of Chemistry

---------- 22.10.2004

Prof.Dr. Muhsin ÇİFTÇİOĞLU
Department of Chemical Engineering

---------- 22.10.2004

Assoc.Prof.Dr. Sedat AKKURT
Department of Mechanical Engineering

---------- 22.10.2004

Prof.Dr. Muhsin ÇİFTÇİOĞLU
Head of Interdisciplinary Material Science and
Engineering Program

ACKNOWLEDGEMENTS

I would like to express my thanks and gratitude to my research advisor, Asst.Prof. Mehtap EANES, her support, patience and guidance during my master research program.

I would also thank to TÜBİTAK and İYTE Research Foundation for their financial support to our Solid State Chemistry Laboratory. I would also thank to IYTE MAM Researchers for their help in analysis and also thanks to Asst.Prof. Funda DEMİRHAN from Celal Bayar University and Philippe Richard Iseo from Bourgogne Dijon University in France for single X-ray data.

Special thanks to my friends in IYTE for their help. Finally, special thanks to my mom, Nuran Şahin, and my father, Ahmet Şahin, and my engaged, Selma Karacaoğlu, for all of their love and support.

ABSTRACT

Hydrothermal method has proven to be an excellent method for the synthesis of novel metal oxides and vanadates.

This research pertains to the synthesis of novel lead chlorovanadate compound and of a known alkali metal trivanadate compound, KV_3O_8 by hydrothermal method. This method has been used to synthesize many inorganic oxide compounds. Hydrothermal synthesis is the use of aqueous solvents under high temperature and high pressure to dissolve and recrystallize materials. Compounds with interesting structure and physical properties are often obtained from this technique that is known as one of the low-temperature synthesis techniques for solid state compounds.

There are many studies that have been done on oxides in the Pb-V-O systems. There are also many vanadium oxides containing Pb, V, O elements in Pb-V-O system such as $Pb_{1.32}V_{8.35}O_{16.7}$, PbV_6O_{11}, PbV_2O_6, $Pb_2V_3O_{8.5}$, and α-$Pb_xV_2O_5$ bronzes (x = 0.3).

In an attempt to synthesize vanadium oxides at low temperature, we were able to obtain needle shaped yellow crystals of $PbVO_3Cl$. In the nature, there is a kombatite mineral, $Pb_{14}(VO_4)_2O_9Cl_4$, with the same composition of elements.

A new lead chlorovanadate, $PbVO_3Cl$, was obtained from the reaction of $NaVO_3$ and $PbCl_2$ in aqueous solution of $B(OH)_3$. The compound was prepared in an autoclave that was filled with aqueous solution of $B(OH)_3$ and heated at 170^{o}C for 3 days. The compound crystallizes in the space group Pnma of the orthorhombic system with formula units in a cell of dimensions a = 10.022(2) Å, b = 5.2875(11) Å, c = 7.1714(14) Å, $\alpha=\beta=\gamma=$ 90°, V= 380.00(13) Å^3 (T = 293 K). It is composed of square pyramidal $[VO_5]$ chains and $[PbCl]_\infty$ sheets. The edge-sharing VO_5 pyramids with a trans configuration were formed by $[VO_3]_n$ chains. This compound is isostructural to $BaVO_3Cl$ and $SrVO_3Cl$ reported by Borel et.al [58].

The single crystals of a known alkali metal trivanadate compound, KV_3O_8, were also synthesized by hydrothermal method. The compound KV_3O_8 has been prepared by hydrothermal synthesis at 170^o C for 3 days from KVO_3, $PbCl_2$ and in 1.66M of $B(OH)_3$ solution. Its structure crystallizes in monoclinic crystal system with space group P2(1)/m with formula units in a cell of dimensions a = 4.9664(10) Å, b = 8.3600(17) Å, c = 7.5982(15) Å, $\alpha=\gamma=$ 90°, β=96.643(3)^o, V= 313.35(11) Å^3 (T = 293(2) K). The

orange hexagonal plate-shaped crystal, KV_3O_8, consists of a layered structure with V_3O_8 layers consisting of VO_6 octahedra and VO_5 square pyramids.

ÖZ

Hidrotermal yöntemin yeni metal oksit ve vanadatların sentezi için çok iyi bir yöntem olduğu kanıtlandı.

Bu çalışma yeni kurşun klorovanadat bileşiğinin ($PbVO_3Cl$) ve bilinen alkali metal trivanadat (KV_3O_8) bileşiğinin hidrotermal yöntem ile sentezini açıklamaktadır. Bu yöntem birçok metal oksit bileşiğinin sentezinde kullanılmıştır. Hidrotermal yöntem maddeleri çözmek ve kristallendirmek için yüksek basınç ve sıcaklık altında sulu çözeltilerin kullanılmasıdır. İlginç yapısal ve fiziksel özelliklere sahip bileşikler genellikle katı hal bileşiklerinin düşük sıcaklık sentez yöntemlerinden birisi olarak bilinen bu teknik ile elde edilir.

Pb-V-O sistemlerindeki oksitler üzerine yapılan birçok çalışma vardır. Ayrıca Pb-V-O sisteminde Pb, V, ve O içeren $Pb_{1.32}V_{8.35}O_{16.7}$, PbV_6O_{11}, PbV_2O_6, $Pb_2V_3O_{8.5}$, and α-$Pb_xV_2O_5$ bronzes (x = 0.3) gibi birçok vanadyum oksit bulunmaktadır.

Düşük sıcaklıkta vanadyum oksit sentezleme girişimlerinde iğne şekilli sarı $PbVO_3Cl$ kristalleri sentezlendi. Doğada aynı elementlere sahip kombatite ($Pb_{14}(VO_4)_2O_9Cl_4$) adlı mineral bulunmaktadır.

Yeni kurşun klorovanadat ($PbVO_3Cl$) $NaVO_3$ and $PbCl_2$'nin borik asit sulu çözeltisindeki reaksiyonundan elde edildi. Bu bileşik borik asit çözeltisi ile dolu otoklav içerisinde hazırlandı ve 170^{o}C de 3 gün boyunca ısıtıldı. Bileşik Pnma space grubunda ve ortorombik sistemdedir. Hücre boyutları aşağıdaki gibidir: a = 10.022(2) Å, b = 5.2875(11) Å, c = 7.1714(14) Å, $\alpha=\beta=\gamma= 90°$, V= 380.00(13) Å^3 (T = 293 K). $[VO_5]$ kare piramitlerinden ve $[PbCl]_\infty$ tabakalarından oluşmaktadır. Trans konfigürasyonlu kenar paylaşımlı VO_5 piramitleri $[VO_3]_n$ zincirlerinden oluşmaktadır. Bu bileşik daha önce Borel ve arkadaşları tarafından belirtilmiş olan $BaVO_3Cl$ and $SrVO_3Cl$ ile izoyapısaldır [58].

Ayrıca bilinen alkali metal trivanadat bileşiğinin single kristalleride (KV_3O_8) hidrotermal yöntem ile sentezlendi. KV_3O_8 bileşiği KVO_3 ve $PbCl_2$ karışımının 1.66M'lık $B(OH)_3$ çözeltisindeki 170^o C de 3 gün süren reaksiyonu sonunda elde edildi. Space grubu P2(1)/m, kristal sistemi ise monokliniktir. Hücre boyutları aşağıdaki gibidir: a = 4.9664(10) Å, b = 8.3600(17) Å, c = 7.5982(15) Å, $\alpha=\gamma= 90°$, β=96.643(3)^o, V= 313.35(11) Å^3 (T = 293(2) K). Hekzagonal şekilli turuncu KV_3O_8 kristalleri

oktahedral VO_6 ve kare piramidal VO_5 içeren V_3O_8 katmanlarından oluşan katmanlı bir yapıya sahiptir.

TABLE OF CONTENTS

LIST OF TABLES

LIST OF FIGURES

CHAPTER 1

INTRODUCTION

1. 1 Definition of Hydrothermal Synthesis

In spite of the fact that the hydrothermal technique has made great progress, there is no unanimity about its definition. The term *hydrothermal* usually refers to any heterogeneous reaction in the presence of aqueous solvents or mineralizers under high pressure and temperature conditions to dissolve and recrystallize materials that are relatively insoluble under ordinary conditions.

There are many different definitions for hydrothermal synthesis in the literature. For instance, Rabenau (1985) defined hydrothermal synthesis as the heterogeneous reactions in aqueous media above 100^{o}C and 1 bar [1]. According to Laudise (1970), hydrothermal growth means growth from aqueous solution at ambient or near-ambient conditions [2]. Lobachev (1973) defined it as a group of methods in which crystallization is carried out from superheated aqueous solutions at high pressures [3].

Roy (1994) declares that hydrothermal synthesis involves water as a catalyst and occasionally as a component of solid phases in the synthesis at elevated temperature (> 100^{o}C) and pressure (greater than a few atmospheres) [4]. Byrappa (1992) defines hydrothermal synthesis as any heterogeneous reaction in an aqueous media carried out above room temperature and at pressure greater than 1 atm [5]. Yoshimura (1994) defines it as reactions occurring under the conditions of high temperature-high pressure (> 100^{o}C, > 1 atm) in aqueous solutions in a closed system [6].

All the above definitions are good for material synthesis. However, there is no definite lower limit for the temperature and pressure conditions. The majority of the authors fix the hydrothermal synthesis at above 100^{o}C and above 1 atm. According to the all definitions, hydrothermal reaction can be described as “any heterogeneous

chemical reaction in the presence of a solvent (whether aqueous or nonaqueous) above room temperature and at pressures greater than 1 atm in a closed system" [7].

1.2 History

The hydrothermal technique has been most popular, garnering interest from scientists and technologists of different disciplines, particularly in the last fifteen years. The *hydrothermal* term is primarily of geological origin, pertaining to the natural processes characterized by joint action of heat and water under pressure. It was first used by the British Geologist, Sir Roderick Murchison (1792-1871), to describe the action of water at elevated temperature and pressure in bringing about changes in the earth's crust leading to the formation of various rocks and minerals [8]

A majority of the minerals formed in the presence of water at elevated temperature and pressure conditions are called "of hydrothermal origin". This contains a huge number of mineral species including ore deposits.

It is well known that the largest single crystals formed in nature and some of the largest quantities of single crystals made by man in one experimental process (quartz crystals of 1000 kg) are both of hydrothermal origin. A number of minerals have formed under hydrothermal conditions over 100^{o}C and 1 bar [9]. With the understanding of the mineral formation in nature under elevated pressure and temperature conditions in the presence of water, the hydrothermal technique has developed.

The first hydrothermal synthesis was carried out in 1845 by Schafhault to obtain quartz crystals upon transformation of freshly precipitated silicic acid in Papin's digestor [10]. Thus, Geologists and mineralogists have determined the conditions needed for the mineral formation in the laboratory during simulations [11].

The first purposeful man-made hydrothermal chemical reaction was probably performed by the German chemist Robert Wilhelm Bunsen in 1839. He contained aqueous solutions in thick walled glass tubes at temperatures above 200^{o}C and at pressures above 100 bars. The crystals of barium carbonate and strontium carbonate that he formed under these conditions marked the first use of hydrothermal aqueous or other solvents as reaction media [12]. This work was followed by that of deSenarmont, He investigated the synthesis of various crystalline solids in superheated water sealed in glass ampoules and counter-pressured in welded gun barrels [13]. The early work was

so productive, and more than 80 types of known minerals were prepared from various recipes in water above its boiling point. Most of this early work was located in the realm of geochemistry, and workers were able to grow many various known minerals, including oxides, silicates, phosphates and sulfides under hydrothermal conditions [14].

During this period, two important achievements appeared. One was the development of the Morey vessel. Morey's development allows hydrothermal fluids to be contained in autoclaves lined with an inert metal, such as silver, gold or platinum, at pressures up to 800 bar [15]. The other was invention of the Bridgeman seal by the great Percy Bridgeman. This invention allowed solutions to be contained at much higher pressures up to 7 kbar [16]. Both of these inventions are used in much the same form today.

After World War II, the hydrothermal method became important for industrial growth of extremely pure crystals with interesting physical properties [17]. Today there are several dozen companies throughout the world that produce α-quartz commercially more than 500 000kg each year [18]. Improvements in electronic industry required new materials, especially as a single crystal, and this necessity made hydrothermal method important.

The first successful commercial application of hydrothermal technology began with mineral extraction or ore beneficiation in the 19th century [19]. The commercial importance of the hydrothermal technique for the synthesis of inorganic compounds was realized with the beginning of the synthesis of large single crystals of quartz [20] and zeolites [21].

The hydrothermal technique has captured the attention of scientists and technologists from different branches of science. Today it is a highly interdisciplinary subject and the technique is popularly used by geologists, biologists, physicists, chemists, ceramists, hydrometallurgists, material scientists, engineers, and so on [7].

Figure 1.1 shows the number of publications year-wise and this number is increasing sharply with the entry of scientists from other branches of science.

As evident from Figure 1.2, the preparative chemists and ceramists have dominated this field, particularly with the recent advances in the advanced materials and electronic ceramics. It is interesting to note that the hydrothermal technique of material synthesis has gained its momentum during the postwar period, although began in the 19th century. Prior to that, majority of the compounds synthesized under hydrothermal

conditions were essentially the natural analogues, as the main thrust was on the study of the origin of rocks, minerals and ores through laboratory simulations.

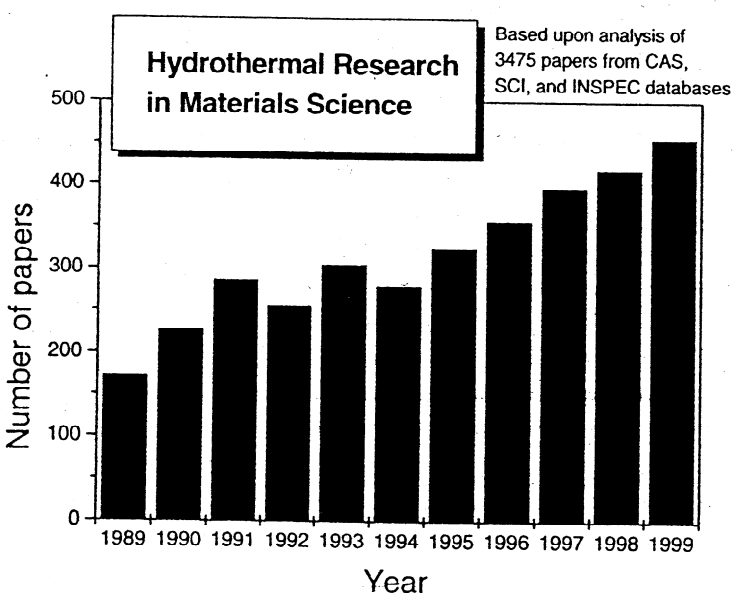

Figure 1.1 Number of publications year-wise.

With the availability of the improved equipment and also with the knowledge on the preparative chemistry routes to synthesize many inorganic compounds, with or without natural analogues under hydrothermal conditions, the popularity of the technique grew fast. Today, the number of compounds without any natural analogue synthesized under hydrothermal conditions is more than the number of compounds with natural analogues synthesized. With the advent of new mineralizers, a wide variety of organic and inorganic compounds until now unknown are being prepared by hydrothermal technique. The technique is being popularly used for crystallization of materials, crystal growth, and materials processing, and so on.

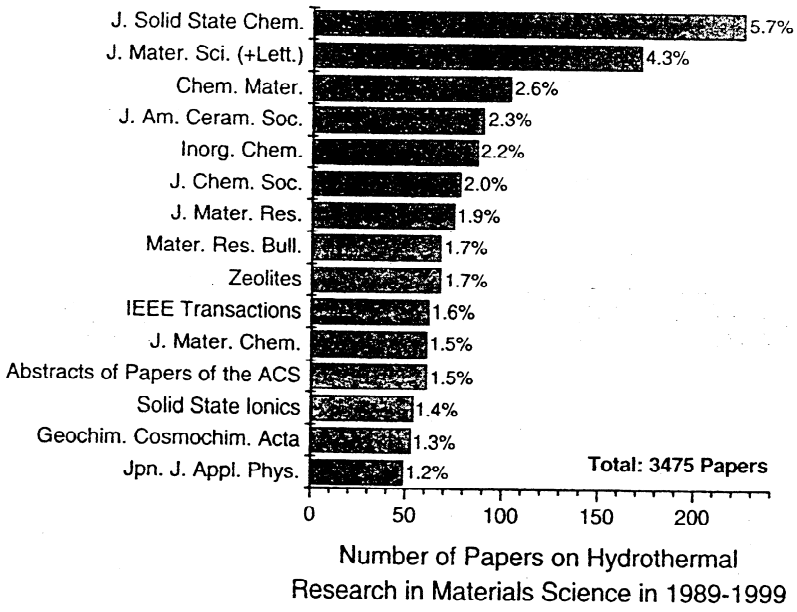

Figure 1.2 Number of papers on hydrothermal research in materials.

1.3 Properties of Hydrothermal Solvents

Most of the inorganic solids are prepared by the reaction of a solid with another solid, a liquid (melt) or a gas, usually at high temperatures. Many "solid/solid" reactions are actually "solid/liquid" reactions, because at the high reaction temperature one of the solid can melt to form liquid phase. Therefore it is sometimes difficult to determine what physical phases are involved in a given reaction.

Solids do not react with each other at room temperature, high temperatures are required to reach the suitable reaction rates. The reason [22] for using high temperature mainly is that if there is a large difference between the structure of the starting material and the product, all bonds in the starting material must be broken, and atoms must migrate before new bonds can be formed. This diffusion makes the reactions impossibly slow unless very high temperatures are used. As a rule of thumb two-thirds of the melting temperature of one component is enough to activate diffusion sufficiently and hence to enable the solid state reaction [23]. Most compounds made at high temperature are thermodynamically very stable. Because thermodynamically stable known phases cannot be avoided, the synthesis of new materials becomes difficult at high

temperatures [24]. However synthesis of new kinetically stable or metastable compounds can be possible if the proper reaction conditions can be found. Preparation of kinetically stabilized compounds requires relatively lower temperatures because the desired compounds are not thermodynamically stable.

Hydrothermal solvents have different properties at above 100^{o}C and above 1 atm, especially at critical point. In order to understand hydrothermal reactions the properties of solvent under hydrothermal conditions must be known very well.

In the Figure 1.3, the critical point marks the end of liquid-vapor coexistence curve at the critical temperature, T_c, and pressure, P_c, in a phase diagram for a pure homogenous substance. A fluid is defined as being supercritical if it is maintained at conditions above its critical temperature and pressure. The properties of supercritical fluids (SCFs) vary depending on the pressure and temperature and frequently described as being intermediate between those of a gas and a liquid. As the temperature increases, the liquid becomes less dense due to thermal expansion and at the same time the gas becomes denser. At the critical point the densities of both phases become the same. The compound is neither liquid nor gas any longer above the critical point, and it becomes supercritical fluid. After that, the phases of liquid and gas are not distinguishable and properties of SCF will be between gas and liquid.

The dielectric constant that is defined as the ability of a solvent to charge separate increases sharply with the pressure in the compressible region that refers to the area around the critical point in which compressibility is considerably greater than would be forecasted from the ideal gas law. This behavior is also parallel to a change in density, as shown in Figure 1.4. Density changes sharply but continuously with pressure in the compressible region. One of the most important advantages of hydrothermal solvents is that a change in density affects the solvating power. A decrease in the density results in a significant change in solvating ability.

Diffusivity and viscosity symbolizes transport properties that influence rates of mass transfer. These features are at least an order of magnitude higher and viscosity is lower compared with a liquid solvent. This means that diffusivity of species in SCF will occur faster than that obtained in a liquid solvent, which means that solids can dissolve and migrate more rapidly in SCFs. High diffusivity, low viscosity and intermediate density increases the rate of the reaction [25, 18].

The low viscosity and high mobility of supercritical water allows it to be excellent reaction media for the synthesis of unique metastable phases and the growth of good quality single crystals for analysis. Superheated water has the ability to solvate reagents and is a good reaction media for better transport and for intermixing of reagents.

Conditions between 100-150^{o}C and 150-375^{o}C are called superheated and hydrothermal, respectively. The properties of hydrothermal solutions carry its characteristics as the same as its supercritical state.

All properties mentioned above allow us to synthesize new good crystals. During this work, all experiments were carried out in the temperature range between 170-200^{o}C.

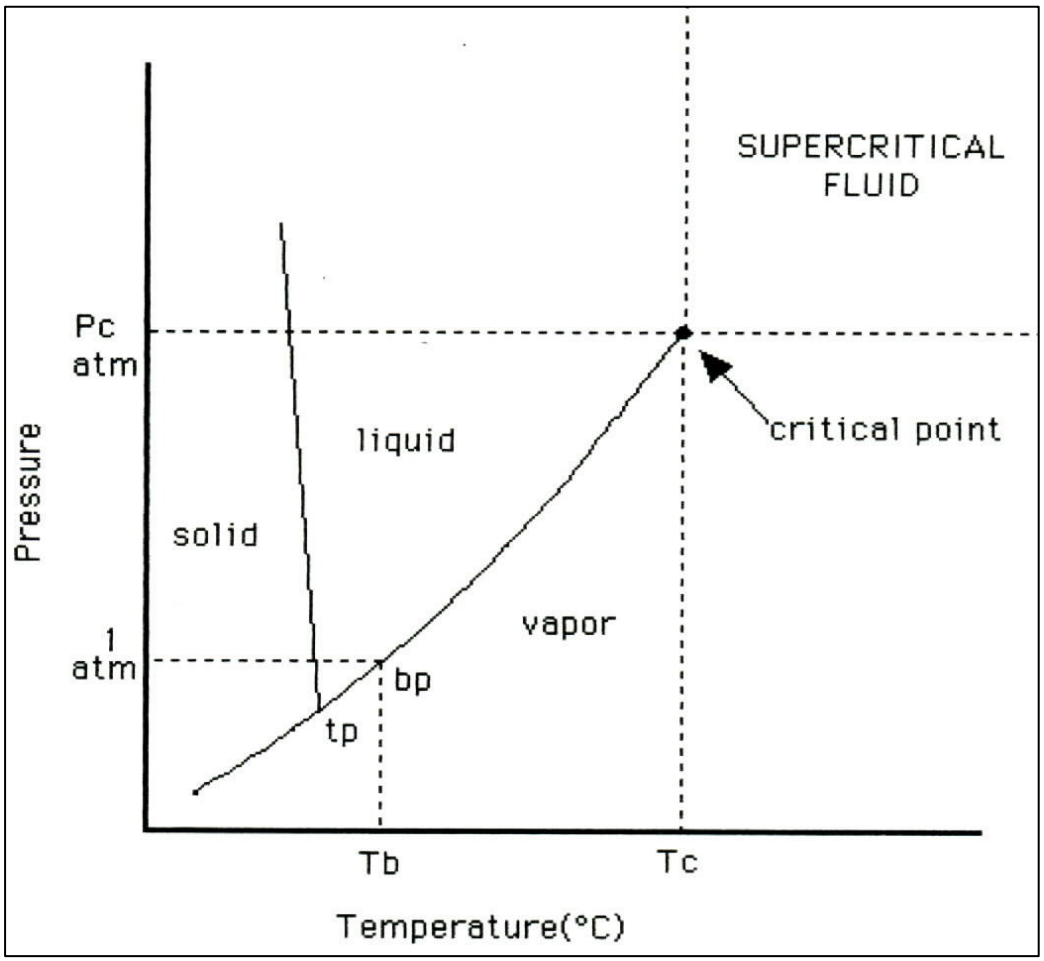

Figure 1.3 Phase diagram of water.

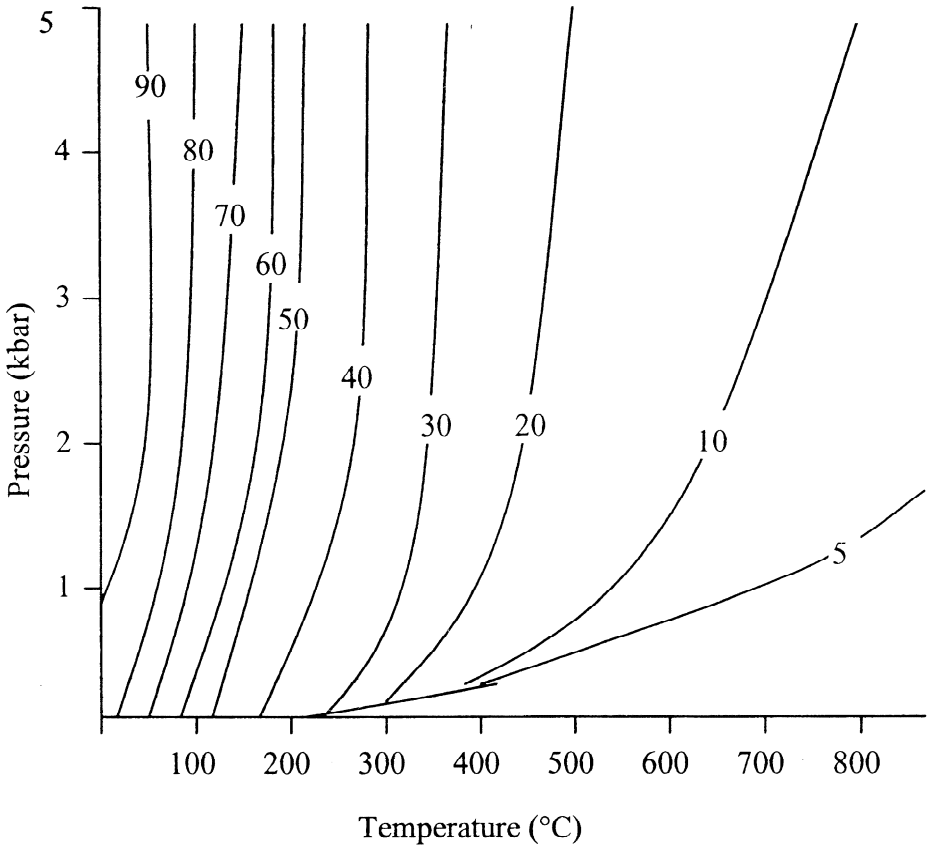

Figure 1.4 Variation of dielectric constant of water with temperature and pressure.

1.4 Water as a Reaction Medium in Hydrothermal Synthesis

Water is one of the most important solvents in nature, and has remarkable properties as a reaction medium under hydrothermal conditions where it acts very differently from water at standard conditions.

One of the biggest advantages of using water is the environmental benefit and cheaper than other solvents, and it can act as a catalyst for the formation of desired materials by tuning temperature and pressure. It is nontoxic, nonflammable, noncarcinogenic, nonmutagenic, and thermodynamically stable. Another advantage is that water is very volatile, so it can be removed from the product very easily [25].

The physical and chemical properties of water and aqueous solutions in the temperature and pressure ranges required for hydrothermal synthesis have been discussed in numerous review articles and are well known. The PVT data for water up

to 1000^{o}C 10 kbar are known accurately enough (within 1% error) [26]. Ion product increases sharply with pressure and temperature. At very high PT conditions (150-200 kbar and 1000^{o}C), water is completely dissociated into H_3O^+ and OH^- , behaving like a molten salt, and has a higher density of the order of 1.7-1.9 g/cm^3. If the density of water is high enough, nonpolar compounds may be completely miscible with it because water behaves as a nonaqueous fluid. Water is a polar solvent and its polarity can be controlled by temperature and pressure and this can be an advantage over other solvents.

For experimental hydrothermal synthesis, to understand the PT behavior of water, it is first necessary to know how it behaves under various conditions of pressure, volume, and temperature. A detailed study of pressure-temperature behavior of water was reported by Laudise [27]. If the autoclave is filled initially to 32%, the liquid level remains until the critical temperature (as shown in Figure 1.5). At the critical point of water, the density of both the gas and liquid is 0.32 g/cm^3. When filled more than 32% with water, the autoclave is filled at temperatures before critical temperature.

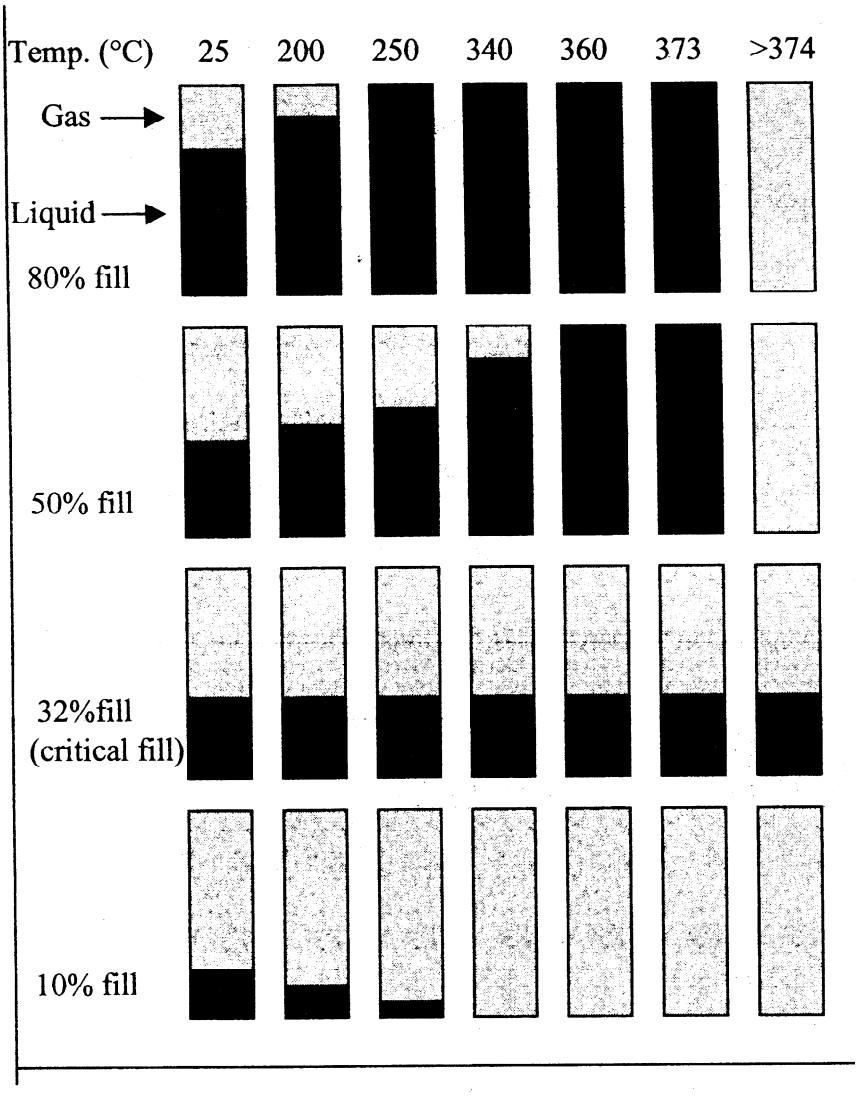

Figure 1.5 Presentation of the P-T behavior of water at various degrees of fill.

When filled less than 32%, the liquid level drops as temperature rises and gas fills the autoclave at temperatures below critical temperature and liquid is lost. The higher percentage of fill, the lower the temperature at which the autoclave becomes filled with liquid [27].

Usually, in most routine hydrothermal experiments, the pressure prevailing under the working conditions is determined by the degree of filling and the temperature.

1.5 Advantages of Hydrothermal Synthesis

There are several advantages of hydrothermal method over conventional solid state. For example, compounds that have elements with an unusual oxidation state can be synthesized such as the formation of ferromagnetic chromium (IV) oxides [1].

$$Cr_2O_3 + CrO_3 \xrightarrow[H_2O]{350^oC,\ 440\ bar} 3CrO_2$$

The hydrothermal method is also useful for synthesis of low temperature phases and metastable compounds by simply using quartz ampoules.

Although hydrothermal synthesis is considered as a high temperature technique, in reality these temperatures are low compared to most traditional melt techniques. There are many important advantages of low temperature crystal growth. For example, it allows the growth of low temperature polymorphs that are often difficult or impossible to prepare by other synthetic methods. The most well known example is α-quartz. Alfa quartz is the most intensively studied material grown hydrothermally in industry for its piezoelectric properties and application in electronic devices. Piezoelectric α-quartz is only stable below 580^{o}C and must be grown below this temperature. This is a problem for conventional melt or flux crystal growth method.

Another important advantage is that reactions do not require much time compared to conventional methods. For instance, although a solid-state reaction can be performed in a few weeks hydrothermal reaction can be done in a few days.

Hydrothermal synthesis also has the advantage of rapid growth rates because of the rapid diffusion processes. The hydrothermal method is a growth technique from liquid solution, but the viscosity of the liquid is lower. Solubility of a liquid should be high for conventional methods or there will be a rate problem. Under hydrothermal conditions, diffusion is not a problem because of a low viscosity in comparison to viscosity at ambient temperature. The down side of this method is the high-pressure requirement and also difficulty on gathering data. Because of fast diffusion under hydrothermal conditions, super saturation occurs and results in dendritic growth that increases the chance of impurities and can reduce crystal quality. The diffusion is fast

even for materials that have low solubility at ambient temperature. For example, quartz cannot be grown at low temperature, however under hydrothermal conditions; it can be grown at relatively high rates [25].

Hydrothermal synthesis is a technique that involves the growth of materials from aqueous solutions at elevated temperature and pressures. Temperature, pressure, and mineralizers are used in this process to increase precursor solubility and to change solution conditions to favor formation of the desired phase. Mineralizers are complexing agents that act to increase the solubility of the starting precursors by forming soluble complexes. This route has several advantages including simplicity, low processing temperatures, low cost, high product purity, and the ability to control the particle size [28].

1.6 Industrial Applications of Hydrothermal Method

After World War II, large single crystals of quartz were formed leading to the first major commercial application for hydrothermal synthesis. At approximately the same time, synthetic zeolitic materials such as zeolite A and X were grown hydrothermally [28].

The successful commercialization of quartz synthesis encouraged several groups to examine the growth of other compounds under hydrothermal conditions, and several other types of crystals were subsequently prepared commercially using hydrothermal techniques, including $AlPO_4$, $KTiOPO_4$ and emeralds [18].

In the past, investigations in this field were conducted by geologist studying the formation of rocks and minerals formed in the earth's crust at high temperature and pressures [14]. Recently, researchers have utilized this process towards the synthesis of commercially important materials such as quartz [29, 30], zeolites [31].

A variety of materials have been synthesized by the hydrothermal method such as $KTiOPO_4$ [32], tungstates [33], Tl- superconductors [34], layered compounds [35], artificial gems [36, 37], intercalation compounds [38], and zeolites [31].

The use of hydrothermal synthesis is proven to be a useful and relatively flexible tool for the production of a wide range of advanced materials. Some of these have already been commercialized; others are still in development or in the scale-up

stage [39, 40]. Researchers engaged in synthesizing materials have a great interest for hydrothermal synthesis, and they are carrying out their studies efficiently, as illustrated in Table 1.1 [40]

Table1.1 Summary of high performance material applications of hydrothermal synthesis.

Fuction	Material	Application
Electrical Insulator	Al_2O_3	IC circuit substrate
Ferroelectirc	$BaTiO_3$, $SrTiO_3$	Ceramic capacitor
Piezoelectric	$Pb(Zr, Ti)O_3$, α-SiO2	Sensors, transducers, actuators
Semiconductor	$BaTiO_3$, ZnO-Bi_2O_3, transition metal oxides	Thermistors and varistors
Chemical	ZnO, Fe_2O_3, ZrO_2, TiO_2, zeolites	Chemical sensor, catalyst, catalyst substrate, desiccant, gas adsorption/storage
Structural	ZrO_2(TZP), cordierite, Al_2TiO_5, mullite, xonotlite	Automotive, heat exchangers, metal filters, light modulator
Biological	Hydroxyapatite	Artifical bone
Colorant	Fe_2O_3, Cr_2O_3, TiO_2-(Ni,Sb), $ZnFe_2O_4$, aluminates, chromites, cobaltites	Ceramic pigments, paints, plastic colorants
Eletronic conductor	Precious metals and alloys, indium tin oxide	Electrode layers, transparent conductive films

1.7 Crystal Growth

The crystal growth is important for producing suitable single crystals for X-ray diffraction measurements. It has been kept general because growing crystals is very much an art, and for any particular substance the method to be chosen and the variations in its use must usually be decided on the basis of exploratory experiments. While initial attempts to grow crystals may be disappointing, it should not be surprising that a number of compounds that at first seemed incapable of producing satisfactory crystals did yield them when the proper conditions were found.

The hydrothermal method of crystal growth has several advantages. It has critical importance for the technological efficiency in developing bigger, purer, and dislocation-free single crystals. The method has been widely accepted since 1960s and practically all inorganic species, starting from native elements to the most complex oxides, silicates, germanates, phosphates, chalcogenides, carbonates, and so on, have been obtained by this method. The technique is being employed on a large scale to prepare piezoelectric, magnetic, optic, ceramic and a host of other materials both as single crystals and polycrystalline materials.

Crystals may be grown from solid, liquid (melt), vapor and solution phases although, usually, only the vapor and liquid phases give crystals of sufficient size to be used in applications or for property measurements. Main categories of crystal growth methods are, growth from the solid: S-S process involving solid-solid phase transition, growth from the melt: L-S process involving liquid-solid phase transition, growth from the vapor: V-S process involving vapor-solid phase transition and growth from solution.

1.7.1 Solid Growth Techniques

Require atomic diffusion. At normal temperatures such diffusion is usually very slow (except in the case of superionic materials where the small cation is quite mobile). Annealing and sintering - hot pressing are two important solid growth techniques.

1.7.2 Vapor Phase Growth

This method depends on the existence of reversible equilibrium between reactant A, transporting agent B, and gaseous product AB.

$$A\,(s) + B\,(g) \rightleftharpoons AB\,(g)$$

1.7.3 Solution Growth

In contrast to the other methods in which melts solidify to give crystals that have the same composition as the melt, precipitation from solution methods involve the growth of crystals from a solvent of different composition to the crystals. The major advantages of solution method are that it permits crystal growth at a temperature well below the melting point and isothermal conditions with slow growth rates give quality crystals of low defect concentration. The disadvantages of this method are its slow grow rate and contamination by the container or flux. The other types of this method are gel growth, flux growth, molten metal solution growth, organic solution growth, thermal freezing method (Bridgman-Stockbarger), zone melting method, flame fusion method (Verneuil method), Czochralski's method, flux pulling (top seeded solution growth-TSSG) and the aqueous solution growth methods (hydrothermal method).Typically the temperature in a hydrothermal process falls between the boiling point of water and the critical temperature of 374^{o}C, while the pressure reaches 22.1 MPa.

In this thesis, our goal was to synthesize new metal oxides using hydrothermal method. Product was planned to be obtained as single crystals by using the ability of hydrothermal method on good quality single crystal growth.

CHAPTER 2

EXPERIMENTAL METHOD

2.1 Teflon-Lined Acid Digestion Parr Autoclave

The autoclave design used was a Parr acid digestion bomb purchased from Parr Instrument Company. These reaction vessels are lined with a removable Teflon insert and posses a maximum operating temperature and pressure of 250^{o}C and 1800 psi, respectively. The closure design consists of a spring-loaded, broad flanged closure that is sealed by tightening the bomb cap with a hook spanner wrench (Figure 2.1) [41]. Due to the larger coefficient of thermal expansion of Teflon (the liner) versus metal (the material in which the liner is enclosed), the Teflon will expand and contract much more upon heating and cooling cycles than its enclosure material. Therefore, a spring-loaded closure is used to maintain a constant pressure on the Teflon seal during both heating and cooling cycles.

These autoclaves have many important advantages over other reaction vessels such as quartz and steel. For instance, they are completely inert to aqueous base and fluorides, making them a workhorse for the zeolite industry. These are sold by a number of vendors and are inexpensive and easy to handle, and require no special auxiliary equipment. The main disadvantage of these autoclaves is that the fluoropolymer liner will begin to deform and weaken above about 240^{o}C, thus cannot contain fluids approaching true supercritical aqueous fluids. Therefore, they have become the primary vessel for hydrothermal work done below 200^{o}C.

The autoclave must be tested carefully prior to heating. Before using a new PTFE cup and cover, these parts should be heated in a bomb with a charge of pure water. This pre-treating will help to develop the required seals and it may prevent annoying leakage in subsequent procedures. The amount of water used in this pre-

treatment should not exceed 40 percent of the capacity of the cup. Maximum charge for inorganic sample is 1.0 gram. These autoclaves can be heated up to 250^{o}C and 1800 psig pressure

A 23-mL Teflon-lined autoclave (Parr Instruments, model 4749) was used as reaction autoclave. Starting materials were added to Teflon cup. After adding, 9 mL of $B(OH)_3$ was added to Teflon cup to provide about 32% fill. Finally, pieces of autoclave are placed in order. These pieces of autoclave are shown in Figure 2.1. The disc order is so important. Firstly, Corrosion disc (thinner one) is placed and then rupture disc (thicker) is put. After closing the autoclave, it is placed into the Carbolite CWF 1100 (Figure 2.2) furnace for at least 1 day at 170-200^{o}C. After the reaction is completed, the autoclave is allowed to cool in the furnace.

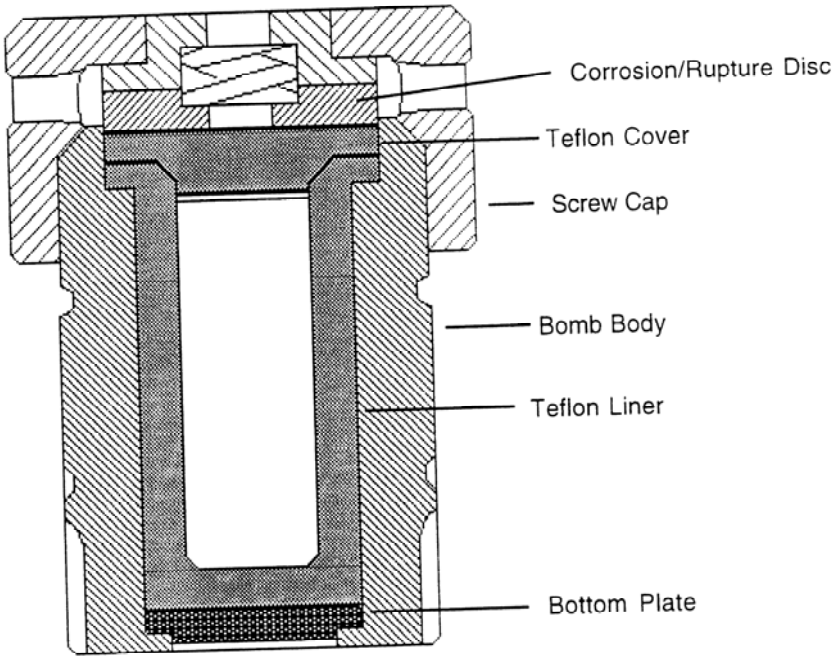

(a)

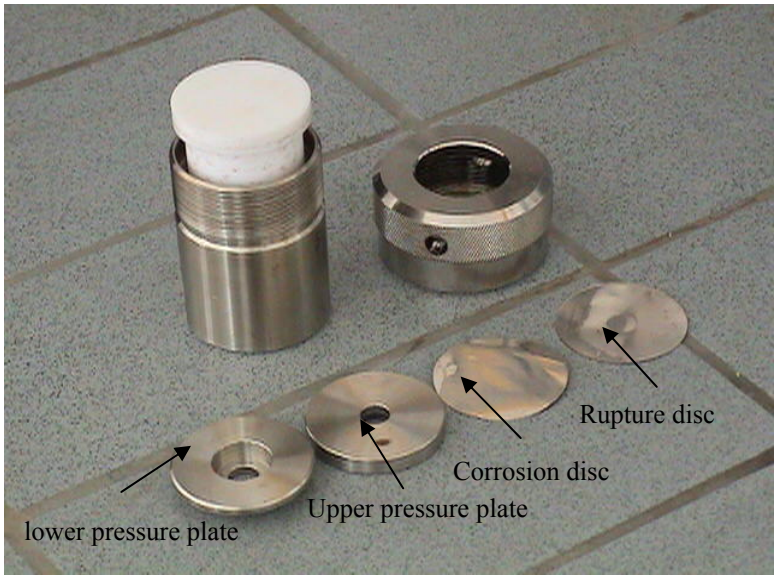

(b)

Figure 2.1 (a) Schematic representation of an autoclave, (b) A Parr acid digestion bomb.

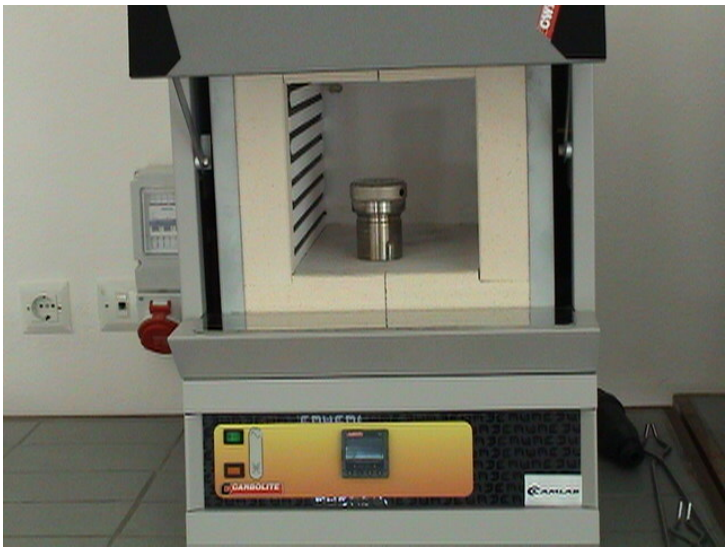

Figure 2.2 Picture of Carbolite CWF 1100 furnace.

2.2 Reagents and Solvents

Boric acid (H_3BO_3, Alfa Aesar 99.99%) was used as the solvent in the reactions. Sodium vanadate ($NaVO_3$, Fluka), and potassium metavanadate (KVO_3, Aldrich 98%) were used as transition metal source. Lead chloride ($PbCl_2$, Riedel-de Haen) was used. Distilled water and acetone were used to wash products.

2.3 Characterization Techniques

The simplest and most obvious first question about an inorganic substance is 'What is it?'. The methods that are used to answer this come into two main categories depending on whether the substance is molecular or non-molecular. If the substance is molecular (whether it is solid, liquid or gaseous), identification is usually carried out by some combination of spectroscopic methods and chemical analysis. If the substance is non-molecular and crystalline, identification is usually carried out by X-ray powder diffraction supplemented, where necessary, by chemical analysis.

Each crystalline solid has its own characteristic X-ray powder pattern which may be used as a 'fingerprint' for its identification. The powder patterns of most known inorganic solids are included search procedure, unknowns can usually be identified rapidly and unambiguously.

Once the substance has been identified, the next stage is to determine its structure, if it is not known already. For molecular materials, further spectroscopic measurements can be used to study the details of the molecular geometry. If the substance is crystalline, X-ray crystallography may be used, in which case information is also obtained on the way in which the molecules pack together in the crystalline state [22].

No single technique is capable of providing a complete characterization of a solid. There are three main categories of physical technique that may be used to characterize solids; these are diffraction, microscopic and spectroscopic techniques. In addition, other techniques such as thermal analysis, physical property measurements may give good information.

2.3.1 X-ray Powder Diffraction

X-ray diffraction methods are some of the most powerful characterization tools known by scientists. In chemistry concerning solids, the two primary pieces of information most often sought are the structure of the material and its reactivity. X-ray diffraction methods can be used to study single crystals, powders and other forms of solids [42].

An X-ray powder diffraction pattern is a set of lines or peaks, each of which are in different intensity and position (d-spacing or Bragg angle, θ) on a strip of photographic film or chart paper. For a given substance the line positions are fixed and characteristic for that substance. The intensities may vary from sample to sample depending on the method of sample preparation and the instrument conditions.

If the substance is a common type then the experimental X-ray powder diffraction pattern can be compared to known published patterns such as those found in the ASTM (American Society for Testing and Materials) tables [42]. Standard patterns of crystalline substances are given in the Powder Diffraction File, JCPDS (Joint Committee on Powder Diffraction Standards) or ASTM File. The inorganic section of this file now contains over 35000 entries and is increasing at a rate of about 2000 per year [22]. If a powder pattern has never been collected before, analogies to known structural types can be made.

X-ray powder diffraction pattern of the compound synthesized were obtained by using a Philips X'pert Pro X-ray diffractometer. Samples were placed on a zero-background silicon sample holder. Data was collected by using CuKα (λ =1.5406 Å) radiation at settings of -45 kV and 40 mA for 30 minutes. The scan rate was 0.1^{o}/sn and the data was collected for 2θ values of 5 to 65^{o}.

2.3.2 Single Crystal X-Ray Diffraction

Single crystal X-ray diffraction methods have several applications such as determination of unit cell and space group, crystal structure determination, electron distribution, atom size and bonding, crystal defects and disorder. The role that crystal structure determination by X-ray diffraction has played in inorganic and solid state

chemistry cannot be exaggerated. Virtually all our knowledge of crystal structures has been obtained by this method over a period of some sixty years. This knowledge has been essential to understand crystalline materials, their structures, properties and applications.

Crystal quality is probably the single most important factor in determining the final precision for a given structural investigation. High-precision structural results require high-quality crystals. In general, crystals should meet the following criteria:

1. They must be single. The crystal should be a single entity which has no smaller crystals or powder attached to it.
2. They must be of the proper size and shape. The crystal should be 0.1 to 0.6 mm. on an edge and as equidimensional as possible. For substances which do not contain highly absorbing elements (e.g. most organic molecules), the optimum sample would be a ~0.5mm. diameter sphere. Needle- or plate-shaped crystals can usually be used if they are at least 0.1mm thick.
3. Good single crystals usually have well-defined and lustrous faces; they are of uniform color and contain no cracks or fracture lines.
4. They must be ordered and diffract to reasonably high scattering angles.
5. They must have reasonably uniform and small mosaic spreads.

Suitable single crystals were mounted in epoxy, and placed in a capillary. Single crystal X-ray diffraction data were collected on a Bruker Smart 1000 CCD diffractometer under following conditions. A full reciprocal sphere corresponding to a total of 3x606 frames collected (ω-scan, 15 s per frame, 0.3^{o} oscillations for 3 different values of j). Monochromatic MoKα (λ=0.71073 Å) was employed. Cell refinement and data reduction were carried out with the use of the program SAINT [43]. Face-indexed absorption corrections were made with the program XREP [44]. The structures were solved by direct methods with the program SHELXS and refined by full-matrix least squares techniques with the program SHELXL in the SHELXTL-97 [44] suite.

2.3.3 Infrared Spectroscopy

The basis of the IR experiment is to pass infrared radiation through a thin sample of compound and measure which energies of the applied infrared radiation are transmitted by the sample [45].

The infrared absorption spectra of both single crystals and KBr pellets were studied in the range of 4000-400cm^{-1} using a FTIR spectrometer (Nicolet Magna-IR 550). A few milligram of sample was mixed with KBr in approximately a 1:10 ratio to prepare the pellet. The mixture was ground by using mortar and pestle and placed inside a die. Then the die was pressed in hydraulic press for 2 minutes under 6000-psi pressure.

Pellets were then placed inside the spectrometer port and measurements were done. Resolution was optimized to 8cm^{-1} and 32 scans were done. Samples were typically run in transmittance mode.

2.3.4 Electron Microscopy (SEM/EDX)

The Scanning Electron Microscope (SEM) has become one of the most widely utilized instruments for material characterization. The SEM is a microscope that uses electrons rather than light to form an image. The SEM has a large depth of field, which allows a large amount of the sample to be in focus at one time. The SEM also produces images of high resolution, which means that closely spaced features can be examined at a high magnification. Preparation of the samples is relatively easy since most SEMs only require the sample to be conductive

The most common accessory equipped with a SEM is the energy dispersive x-ray detector or EDX. This type of detector allows a user to analyze a sample molecular composition.

Qualitative analysis of the heavy elements in single crystal samples was obtained using a Philips XL 30S FEG Scanning Electron Microscope. The accelerating voltage for each scan was 5 kV with an accumulation time of 30 seconds. Spot was 3, and magnification was 1200. The detector type was Secondary Electron (SE) or Through the Lens (TLD). The results of EDX analysis are usually presented as a spectrum. In this

graphical representation the X -axis represents the energy level - and therefore identifies the elements, and the Y-axis provides the number of counts of each element detected.

2.3.5 Thermogravimetric Analysis (TGA) and Differential Scanning Calorimetry (DSC)

Change in the weight and enthalpy changes of the synthesized compounds with temperature were examined using thermogravimetric analysis (Shimadzu TGA-51), and differential scanning calorimetry (Shimadzu DSC-50), respectively.

For the DSC measurements, powder samples typically in the size of 10-25mg were placed in an aluminum pan. The samples were analyzed at 5^{o}C/min from room temperature to 500^{o}C and then cooled to room temperature with nitrogen flow. Flow rate was 40 mL/min.

For the TGA measurements, powder samples in the size of 10-25mg were placed in a platinum pan. The samples were analyzed at 5^{o}C/min from room temperature to 1000^{o}C with nitrogen flow. Flow rate was 40 mL/min.

CHAPTER 3

SYNTHESIS AND CHARACTERIZATION of KV_3O_8

3.1 Introduction

Vanadium compounds are extensively studied because of their interesting redox, electrochemical, and catalytic or magnetic properties. For example, among the oxides, the layered lithium vanadates are used as electrode material in lithium batteries [46] [47], whereas the bismuth oxides are good candidates for solid electrolytes in fuel cells [48]. Some other vanadates show catalytic activities in the oxidative dehydrogenation of hydrocarbons [49, 50].

The vanadium oxide part of the hybrid materials has the $V_xO_y^{n-}$ formula. In mineral chemistry, vanadium exhibits three oxidation states V(III), V(IV) and V(V). The coordination polyhedra observed for V(IV) are square pyramidal and distorted octahedral or square bipyramidal. The square pyramidal geometry may be described as 4 + 1. This square pyramidal geometry has one short vanadyl bond in the apical position and four longer equatorial bonds (1.80–2.12 Å). The six-coordinate geometry has been denoted as 4 + 1 + 1, that has four intermediate equatorial bonds (1.86–2.16 Å), one axial vanadyl bond, and a long axial bond (2.20–2.32 Å) (Figure 3.1) [51].

Pentavalent vanadium may exhibit tetrahedral, square pyramidal, distorted trigonal bipyramidal, and distorted octahedral or square bipyramidal geometries. The tetrahedral coordination exhibits bond lengths in the range 1.60 to 2.0 Å. These bond lengths are distributed into short (ca. 1.6 to 1.7 Å) and longer distance (ca. 1.8 to 2.0 Å) depending on the terminal or bridging nature of the V–O bond [51].

The five-coordinate geometry displayed by V(V) reflects the number of vanadyl groups. Thus, when there is a single V=O bond, the 4+1 square pyramidal geometry is observed, while the presence of two short V=O bonds results is distorted trigonal

bipyramidal 3 + 2 geometry, with the short vanadyl bonds occupying two equatorial positions and the longer bonds occupying one equatorial and two axial positions [51].

The six coordinate V(V) polyhedra shows 4+1+1 or 2 + 2 + 2 bond distributions, depending on the presence of one or two short vanadyl bonds, respectively. The 4 + 1 + 1 geometry is similar to that described above for tetravalent vanadium. The 2 + 2 + 2 geometry is defined by two short vanadyl bonds in a cis orientation, two long bonds (2.1–2.3 Å) trans to the vanadyl groups and two intermediate bond lengths (1.85–2.05 Å) cis to the V=O bonds [51].

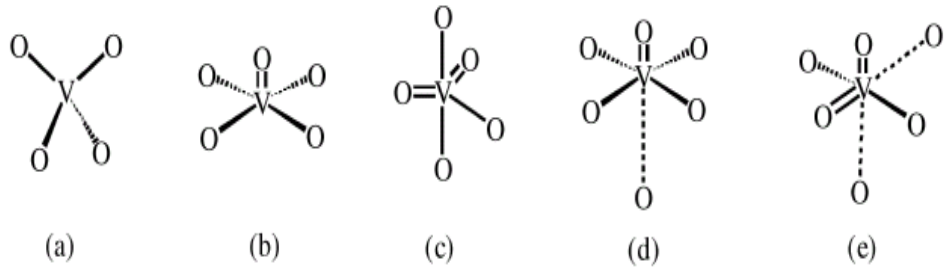

Figure 3.1 Coordination polyhedra adopted by V (V)- and V (IV)- oxo species: (a) tetrahedral, (b) "4 + 1" square pyramidal, (c) "3 + 2" trigonal bipyramidal, (d) "4 + 1 + 1" octahedral, and (e) "2 + 2 + 2" octahedral**.**

Vanadium oxide chemistry is characterized by several general families of compounds: binary oxides, bronzes, and molecular polyanions. The chemistry of polyanions is vast and has been reviewed recently [51, 52]. Representative examples of vanadate cluster chemistry include divanadate, $(V_2O_7)^{4-}$ [53], tetravanadate $(V_4O_{12})^{4-}$ [54] and decavanadate $(V_{10}O_{28})^{6-}$ [55], shown in Figure 3.2. $(V_4O_{12})^{4-}$ structure is a ring of corner sharing V(V) tetrahedra, the decavanadate is constructed from edge-sharing V(V) octahedra. Vanadium polyhedra in both the cluster chemistry and the solid state may show edge-, corner-, and face-sharing.

Metavanadates are characteristic oxides of vanadium which have the empirical formula VO_3^- such as KVO_3 and β-$NaVO_3$ (Figure 3.3). KVO_3 consists of a chain of corner-sharing tetrahedras. In contrast, the structure of β-NaVO3 consists of a double

chain of edge-sharing trigonal bipyramids (2 + 3 geometry), formed by the fusion of two corner-sharing tetrahedral chains [51].

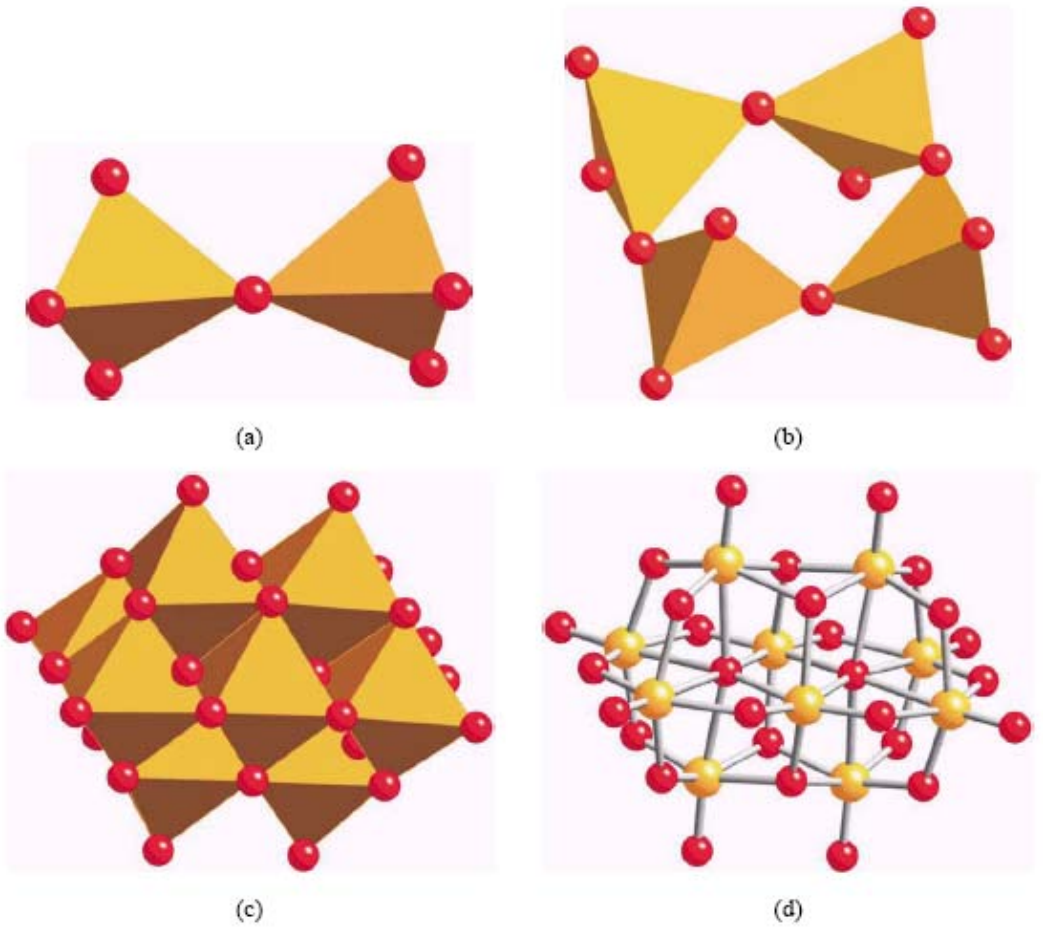

Figure 3.2. Polyhedral representations of the structures of the (a) $[V_2O_7]^{4-}$ and (b) $[V_4O_{12}]^{4-}$ clusters; (c) ball and stick and (d) polyhedral views of the structure of $[V_{10}O_{28}]^{6-}$.

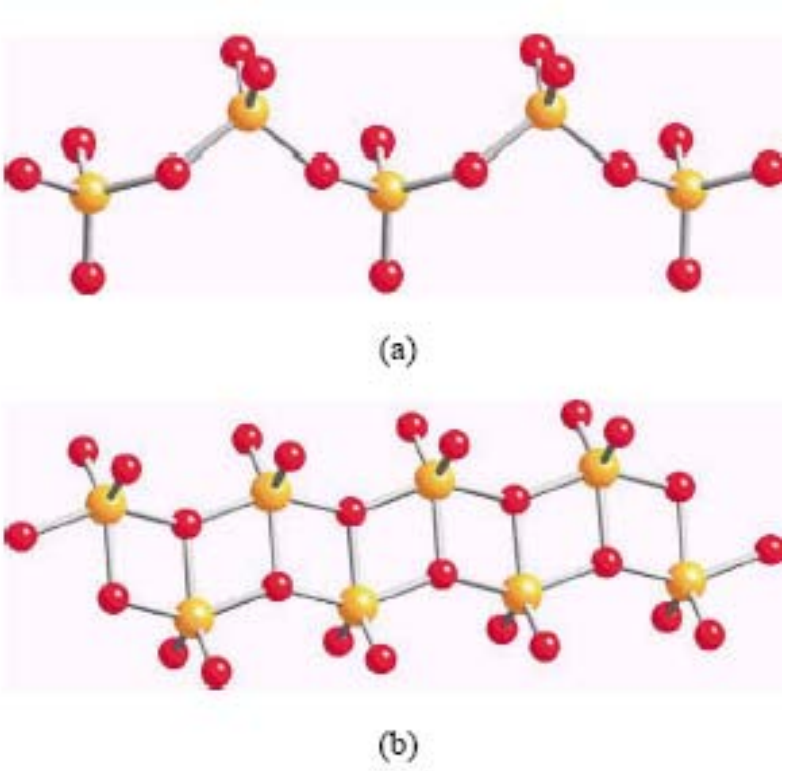

Figure 3.3 Views of the one-dimensional vanadate chains of (a) KVO_3 and (b) β-$NaVO_3$.

The structure of V_2O_5 exhibits characteristic features of two-dimensional vanadium oxides. As shown in Figure 3.4, the structure is constructed from both edge- and corner-sharing of [VO5] square pyramids. The double chains of edge-sharing polyhedra consist of a chain with the apical oxo group directed above the plane of network while the second chain exhibits oxo groups directed below the plane. The layers pack such that there are weak interlayer V–O interactions at 2.79 Å [51].

The title compound has been synthesized by Oka et.al using hydrothermal method with different starting materials in the past. They have applied hydrothermal synthesis for alkali-metal vanadium oxides by using various vanadium and alkali-metal sources. In their work, starting materials for growing AV_3O_8 crytsals were V_2O_5 powders and alkali-metal nitrate $A(NO)_3$ solutions for A= K, Rb, Cs, NH_4. V_2O_5 powders were obtained by the thermal oxidation of $VO(OH)_2$ powders in air, where $VO(OH)_2$ powders were prepared in advance by the hydrothermal treatment of

$VOSO_4$-NaOH slurries. A suspension of 0.5g V_2O_5 powders in 0.2 mol/L ANO_3 solution was sealed in a Pyrex ampoule and treated hydrothermally in an autoclave at 250^{o}C for 48 h. Then, orange transparent crystals were separated by filtration [56].

In contrast to this work, KV_3O_8 crystals were hydrothermally grown at 170^{o}C for 3 days in our laboratory. In this thesis, our goal was to synthesize metal oxide compounds by using hydrothermal method. Here an alkali-metal trivanadate, KV_3O_8, has been synthesized in aqueous solution, structurally characterized, and some of its properties explained. In this section we report the synthesis and structural characterization of KV_3O_8.

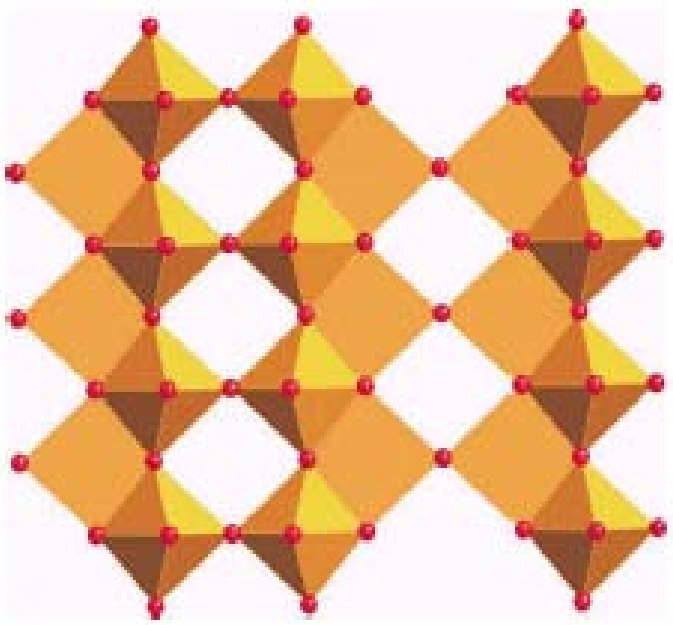

Figure 3.4 The network structure of V_2O_5.

3.2 Experimental Procedure

3.2.1 Synthesis of KV_3O_8

Single crystals of KV_3O_8 were obtained from a reaction mixture of KVO_3 (552.4 mg, 4 mmol), $PbCl_2$ (556.9 mg, 2 mmol). This mixture was loaded into a 23-mL Teflon-lined autoclave. 1.66M of $B(OH)_3$ was added to fill ~ 40% of the total volume. The mixture was heated in an oven at 170^oC for 3 days and then slowly cooled to room temperature.

After cooling, the resulting mixture was opened, and solid products were filtered, washed several times with distilled water and acetone, and finally dried in air at room temperature. The hexagonal plate-shaped orange crystals were obtained in an orange solution as reaction products (Figure 3.5). These hexagonal orange crystals (KV_3O_8) were examined with EDX, and K (12.25%), V(47.15%), O(40.60%) atoms were found in these crystals. ICSCD database was used to check this data. The SEM EDX peaks of KV_3O_8 crystals and the SEM EDX results (weight %) were shown in Figure 3.6 and in Table 3.1, respectively.

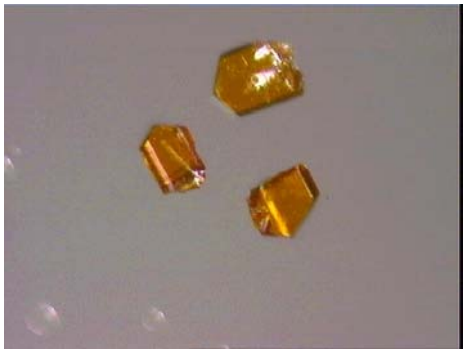

Figure 3.5 Crystal pictures of KV_3O_8 (Nikon Eclips L150 Optic Microscope, 10 X magnitudes).

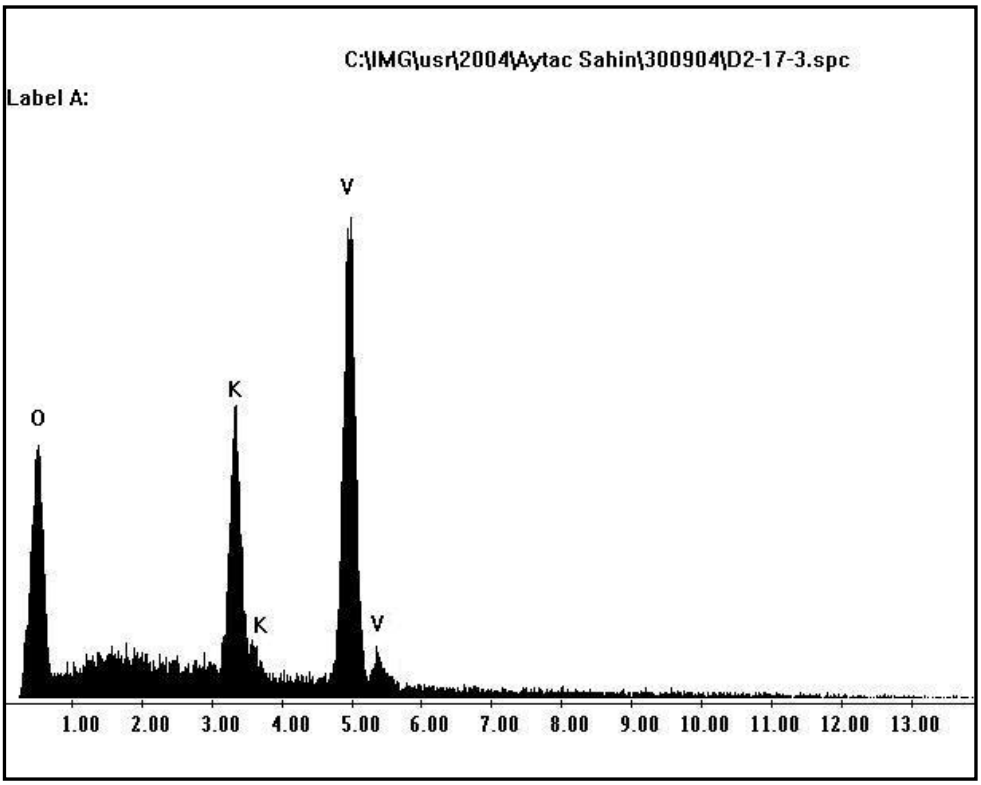

Figure 3.6 The SEM EDX peaks of KV_3O_8.

Tablo 3.1 EDX results of orange plate-shaped crystals (KV_3O_8).

Element	**Weight %**	**Atomic %**
K	12.25	8.30
O	40.60	67.19
V	47.15	24.51
Total	100.00	100.00

In order to synthesize new crystals, many different reactions were performed and two different crystals were obtained. The reaction (1) was the first reaction that was done for this crystal (2:1:15 ratio). The quality of the crystals was not good and yield of

the reaction (approximately 10%) was also not good. In order to increase the yield and the quality of the crystals, similar reactions were tried under the same conditions (at 170^{o}C for 3 days) with different ratios such as (3:1:15), (10:1:30), (5:1:15), (5:2:15). All these reactions gave the same products with better and different yields. Among these reactions the best yield was obtained from the reaction with 3:1:15 ratios (approximately 20%).

$$(2{:}1{:}15)\ KVO_3\ (s) + PbCl_2\ (s) \xrightarrow[170\ ^{o}C \text{ for } 3 \text{ days}]{1{,}66M\ B(OH)_3} KV_3O_8 \qquad (1)$$

After these reactions, we tried to increase the reaction time to obtain the better crystal quality. In order to do this, the reaction (2) with 3:1:15 mole ratio was done at 170^{o}C for 5 days. The increase in the reaction time gave crystals with better quality. After all these reactions, the increase in the reaction temperature was tried, but it did not change either the crystal quality or the reaction yield. After this experiment we saw that the increase in the reaction time was more effective on producing good quality single crystals than the increase in the reaction temperature.

$$(3{:}1{:}15)\ KVO_3\ (s) + PbCl_2\ (s) \xrightarrow[170\ ^{o}C \text{ for } 5 \text{ days}]{1{,}66M\ B(OH)_3} KV_3O_8 \qquad (2)$$

The best reaction yield (approximately 30%) and the best crystal quality were obtained from the reaction (2) with 3:1:15 ratios and 170^{o}C for 5 days.

As mentioned before these crystals were synthesized by Oka et.al with more complicated procedure in 2 days. We wondered if we could obtain these crystals in 1 or 2 days. In order to do this, we tried the following reactions (3:1:15 mole ratio):

$$(3{:}1{:}15)\ KVO_3\ (s) + PbCl_2\ (s) \xrightarrow[170\ ^{o}C \text{ for } 1 \text{ day}]{1{,}66M\ B(OH)_3} KV_3O_8 \qquad (3)$$

$$(3{:}1{:}15)\ KVO_3\ (s) + PbCl_2\ (s) \xrightarrow[170\ ^{o}C \text{ for } 2 \text{ days}]{1{,}66M\ B(OH)_3} KV_3O_8 \qquad (4)$$

Both reactions (3) and (4) gave the same product with different yield. There were a few orange crystals in the reaction (3), however many orange crystals were obtained from the reaction (4).

When looking at the compound, there are not Pb, and Cl atoms in the compound. In order to search the effect of $PbCl_2$ on obtaining the orange crystals reactions (5), and (6) were done.

$$(7{:}15)\ KVO_3\ (s) \xrightarrow[170\ ^oC \text{ for } 1 \text{ days}]{1{,}66M\ B(OH)_3} KV_3O_8 \qquad (5)$$

$$(7{:}15)\ KVO_3\ (s) \xrightarrow[170\ ^oC \text{ for } 2 \text{ days}]{1{,}66M\ B(OH)_3} KV_3O_8 \qquad (6)$$

There were not any crystals in the reaction (5), however many orange crystals were obtained from the reaction (6).

Many reactions have made to get KV_3O_8 crystals by using hydrothermal method. As it is seen when reaction (3) was tried at 170^{o}C for 1 day, a few orange crystals were able to be obtained. However, when the reaction (6) was done without using $PbCl_2$ at 170^{o}C for 2 days, many orange crystals were obtained. In reaction (3) $PbCl_2$ might have acted as mineralizer. It can be said that KV_3O_8 crystals can be synthesized in 1 day with $PbCl_2$, however if $PbCl_2$ does not want to be used due to its being expensive, these crystals cane be obtained in 2 days without using $PbCl_2$ with this method.

3.2.2 X-ray Crystallographic Analyses

A single crystal of KV_3O_8 was mounted with epoxy in a capillary and was placed on a Bruker Smart 1000 CCD diffractometer under following conditions. A full reciprocal sphere corresponding to a total of 3x606 frames collected (ω-scan, 15 s per frame, 0.3^o oscillations for 3 different values of φ). Monochromatic MoKα (λ=0.71073 A^o) was employed. Cell refinement and data reduction were carried out with the use of the program SAINT [43]. Face-indexed absorption corrections were made with the program XREP [44]. The structures were solved by direct methods with the program SHELXS and refined by full-matrix least squares techniques with the program

SHELXL in the SHELXTL-97 [44] suite. Further crystallographic details were given in Table 3.2.

Table 3.2 Crystallographic Data for KV_3O_8

Formula	KV_3O_8
Fw	446.55
Crystal system	Monoclinic
Space group	P2(1)/m
Z	2
a, Å	4.9664(10)
b, Å	8.3600(17)
c, Å	7.5982(15)
$\alpha=\gamma$ deg	90
$\beta=$ deg	96.643(3)
V, $(Å)^3$	313.35(11)
Dcalc, g/cm^3	2.366
μ, mm^{-1}	3.211
2θ range, deg	2.70– 27.53

Atomic coordinates and equivalent isotropic displacement coefficients, and anisotropic displacement coefficients were given in Table 3.3 and Table 3.4, respectively. The bond angles were given in Table 3.5. All bond distances and bond valence were given in Table 3.6.

Table 3.3 Atomic Coordinates ($x10^4$) and Equivalent Isotropic Thermal Parameters of KV_3O_8.

Atom	X	Y	Z	Ueq
V1	0.58113	0.25000	0.41967	0.0042
V2	1.06012	0.05337	0.30764	0.0041
K1	0.5444	0.25000	-0.06579	0.0121
O1	0.9031	0.25000	0.2325	0.0049
O2	0.3776	0.25000	0.5698	0.0083
O3	0.8114	0.0855	0.4942	0.0061
O4	1.3818	0.0971	0.2537	0.0059
O5	0.9303	-0.0706	0.1609	0.0079

Table 3.4 Anisotropic Displacement Coefficients ($Å^2x\ 10^3$) of KV_3O_8.

Atom	U11	U22	U33	U23
V1	0.0026(5)	0.0034(5)	0.0067(5)	0.000
V2	0.0033(5)	0.0029(5)	0.0063(5)	0.00020(19)
K1	0.0097(6)	0.0157(7)	0.0099(6)	0.000
O1	0.0031(16)	0.0041(15)	0.0097(16)	0.000
O2	0.0068(16)	0.0079(17)	0.0097(17)	0.000
O3	0.0045(11)	0.0049(11)	0.0077(12)	0.0005(8)
O4	0.0052(11)	0.0045(11)	0.0080(12)	0.0005(9)
O5	0.0099(14)	0.0057(13)	0.0094(12)	0.0007(9)

Table 3.5 All Bond Angles (degrees) of KV_3O_8.

O2 V1 O3	101.62(13)x2	O3 V1 O3	97.03(17)
O2 V1 O4	98.20(14)x2	O3 V1 O4	87.73(11)x2
O3 V1 O4	158.20(12)x2	O4 V1 O4	80.50(16)
O2 V1 O1	173.95(18)	O3 V1 O1	74.53(11)x2
O4 V1 O1	86.40(10)x2	O2 V1 V2	139.62(9)x2
O3 V1 V2	38.25(9)x2	O3 V1 V2	90.66(9)x2
O4 V1 V2	79.93(8)x2	O4 V1 V2	120.82(9)x2
O1 V1 V2	37.20(5)x2	V2 V1 V2	64.26(3)
O2 V1 V2	67.78(12)x2	O3 V1 V2	162.22(8)x2
O3 V1 V2	99.08(8)x2	O4 V1 V2	80.07(8)x2
O4 V1 V2	30.95(8)x2	O1 V1 V2	117.13(8)x2
V2 V1 V2	148.30(4)x2	V2 V1 V2	106.67(3)x2
V2 V1 V2	64.04(3)	O5 V2 O4	106.24(15)
O5 V2 O1	103.58(14)	O4 V2 O1	96.05(14)
O5 V2 O3	102.81(13)	O4 V2 O3	94.57(12)
O1 V2 O3	147.43(14)	O5 V2 O3	110.34(13)
O4 V2 O3	143.10(12)	O1 V2 O3	80.19(14)
O3 V2 O3	72.95(12)	O5 V2 V1	105.96(10)
O4 V2 V1	135.46(10)	O1 V2 V1	46.61(11)
O3 V2 V1	107.32(8)	O3 V2 V1	34.57(8)
O5 V2 V1	142.19(11)	O4 V2 V1	35.95(9)
O1 V2 V1	85.62(10)	O3 V2 V1	85.15(8)
O3 V2 V1	107.34(8)	V1 V2 V1	106.67(3)
V2 O1 V2	121.96(19)	V2 O1 V1	96.18(12)x2
V1 O3 V2	145.19(16)	V1 O3 V2	107.18(14)
V2 O3 V2	107.05(12)	V2 O4 V1	113.10(14)

3.2.3 Bond Valence Calculations

Table 3.6 Bond Lengths (Å) and Bond Valence (*italic*) in KV_3O_8.

Environment of V(1)			Environment of V(2)		
V(1) – O(1)	2.260(4)	*0.290(3)*	V(2) – O(1)	1.880(2)	*0.812(39)*
V(1) – O(2)	1.609(4)	*1.690(2)*	V(2) – O(3)	1.949(3)	*0.674(6)*
V(1) – O(3)	1.836(3)	*0.914(7)*	V(2) – O(3)	2.003(3)	*0.582(4)*
V(1) – O(3)	1.836(3)	*0.914(7)*	V(2) – O(4)	1.734(3)	*1.205(10)*
V(1) – O(4)	1.979(3)	*0.621(5)*	V(2) – O(5)	1.602(3)	*1.721(13)*
V(1) – O(4)	1.979(3)	*0.621(5)*			
<V(1) – O>	1.916(20)		<V(1) – O>	1.834(14)	
∑ij sij =		*5.05(29)*	∑ij sij =		*4.99(72)*
Environment of K(1)			Environment of O(1)		
K(1) – O(1)	2.716(4)	*0.206(2)*	O(1) – V(2)	1.880(2)	*0.812(39)*
K(1) – O(2)	2.797(4)	*0.166(2)*	O(1) – V(2)	1.880(2)	*0.812(39)*
K(1) – O(4)	2.938(3)	*0.113(1)*	O(1) – V(1)	2.260(4)	*0.290(3)*
K(1) – O(4)	2.938(3)	*0.113(1)*	O(1) – K(1)	2.716(4)	*0.206(2)*
K(1) – O(5)	2.817(3)	*0.157(1)*			
K(1) – O(5)	2.817(3)	*0.157(1)*			
K(1) – O(5)	3.164(3)	*0.061*			
K(1) – O(5)	3.164(3)	*0.061*			
K(1) – O(4)	3.273(3)	*0.046(1)*			
K(1) – O(4)	3.273(3)	*0.046(1)*			
<K(1) – O>	2.990(32)		<O(1) – V>	2.184(12)	
∑ij sij =		*1.125(10)*	∑ij sij =		*2.12(83)*
Environment of O(2)			Environment of O(3)		
O(2) – K(1)	2.797(4)	*0.166(2)*	O(3) – V(2)	1.949(3)	*0.674(6)*
O(2) – V(1)	1.609(4)	*1.690(2)*	O(3) – V(2)	2.003(3)	*0.582(4)*
			O(3) – V(1)	1.836(3)	*0.914(7)*
< O(2) – K>	2.203(8)		< O(2) – K>	1.929(9)	
∑ij sij =		*1.856(4)*	∑ij sij =		*2.17(17)*
Environment of O(4)			Environment of O(5)		
O(4) – V(1)	1.979(3)	*0.621(5)*	O(5) – K(1)	2.817(3)	*0.157(1)*
O(4) – V(2)	1.734(3)	*1.205(10)*	O(5) – K(1)	3.164(3)	*0.061*
O(4) – K(1)	3.273(3)	*0.046(1)*	O(5) – V(2)	1.602(3)	*1.721(13)*
O(4) – K(1)	2.938(3)	*0.113(1)*			
< O(4) – K>	2.481(12)		< O(5) – K>	2.528(9)	
∑ij sij =		*1.985(17)*	∑ij sij =		*1.939(14)*

The parameters needed to calculate bond valences from bond lengths have been determined for 750 atom pairs by using Inorganic Structure Database. The 141 most reliable values are listed in Ref 52.

The results refer to the equation $\sum s(M\text{-}L) = \sum \exp[(r_o - r)/0.37]$ with r_o= 1.803(3)Å, 2.132(4)Å for V^{5+}-O, K^{1+}-O, respectively [57]. V^{5+}-O, K^{1+}-O distances are from the table in reference 52. This equation is given which allows the calculation of the remainder as well as the calculation of parameters for over a thousand other bond types.

s= individual bond valences, r = bond distances in structure and r_o = empirically derived single M-L bond distance in angstrom.

3.2.4 Results and Discussion

The compound having the formula KV_3O_8 was prepared from the reaction of KVO_3: $PbCl_2$ in boric acid as orange hexagonal plate-shaped crystals. KV_3O_8 adopts a layered structure with V_3O_8 layers consisting of VO_6 octahedra and VO_5 square pyramids. In figure 3.7, the unit cell of KV_3O_8 is viewed down the a-axis. The title compound has two unique vanadium atoms (V1, V2) with different coordination environment.

The V1 has a distorted octahedral environment and it coordinates to six O atoms at distances in the range of 1.609(4)– 2.260(4)Å. The V2 has a square pyramidal coordination environment with the apical oxygen at a distance of 1.602(3)Å and four basal oxygens at distances in the range of 1.734(3)– 2.003(3)Å. In figure 3.8, coordination environment of V1 and V2 atoms with O atoms were shown. $V(1)O_6$ octahedra shares four corners and two edges with $V(2)O_5$ square pyramids. In addition to this, $V(2)O_5$ shares one corner and one edge with $V(2)O_5$ square pyramid, and two corners, one edge with $V(1)O_6$ octahedra. In figure 3.9, polyhedral representations of VO_6 octahedras and VO_5 square pyramids were shown.

Valence sum calculations indicate that all V are pentavalent, all oxygens are divalent, and K atom is monovalent. This oxidation state is consistent with the overall charge balance of the compound. The square pyramidal vanadium and octahedral vanadium have an oxidation state of +5. As shown from Table 3.6, this assignment of oxidation state is confirmed by the valence sum calculations which gave value of

5.05(29) and 4.994(72) for V(1), and V(2) atoms , respectively. .As mentioned before, the pentavalent vanadium atoms can adopt various environments such as octahedral, pyramidal, and tetrahedral. Two configurations are observed in $V^{v}O_6$, either 2+2+2 or 4+1+1. In the title compound, $V^{v}O_6$ octahedra has 4+1+1 configuration as shown in figure 3.1d, and $V^{v}O_5$ polyhedra has also 4+1 configuration as shown in figure 3.1b. Interlayer K atoms are sandwiched by $V(1)O_6$ octahedral faces (Figure 3.10).

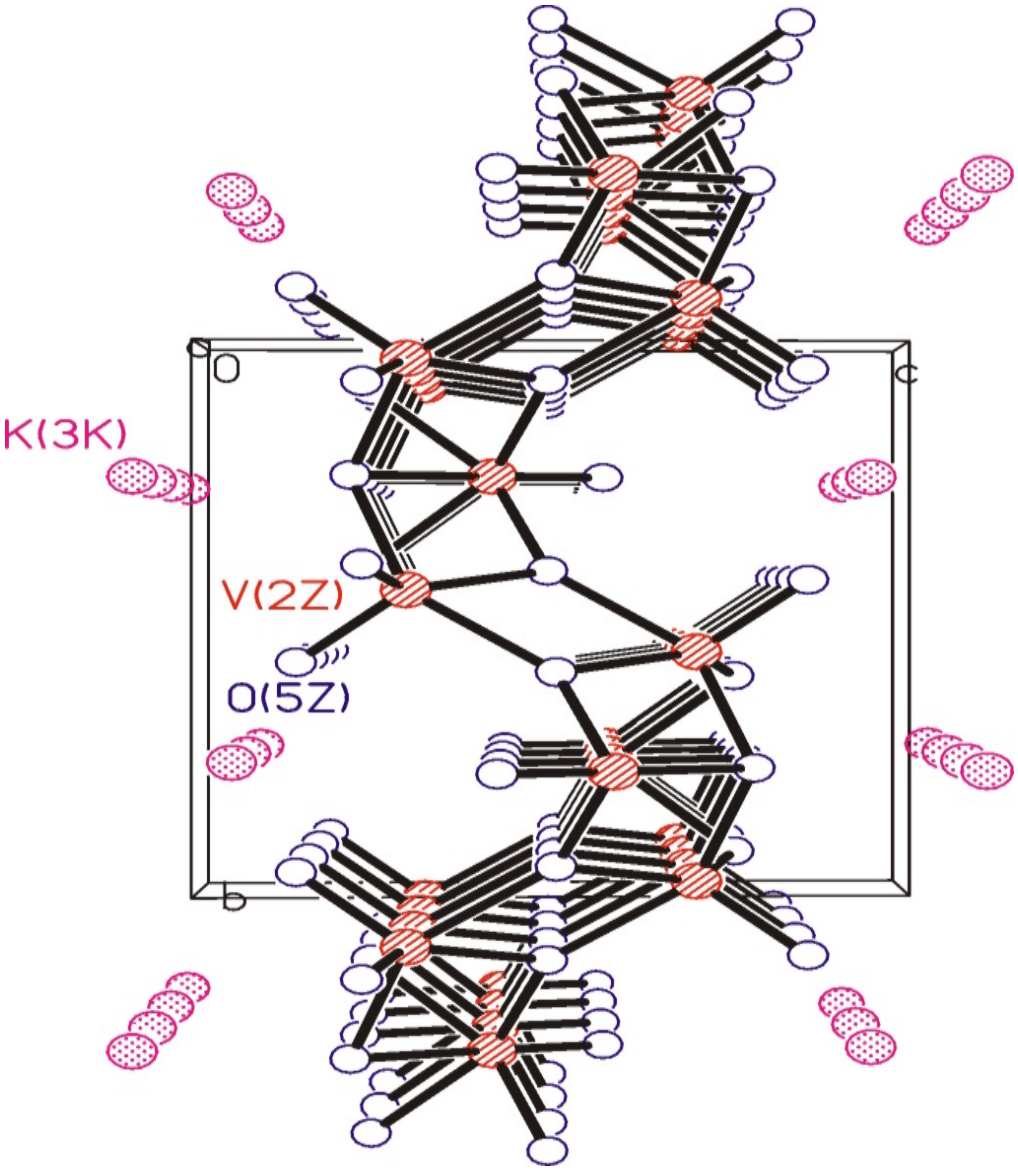

Figure 3.7 Unit cell view of KV_3O_8 running along a axis.

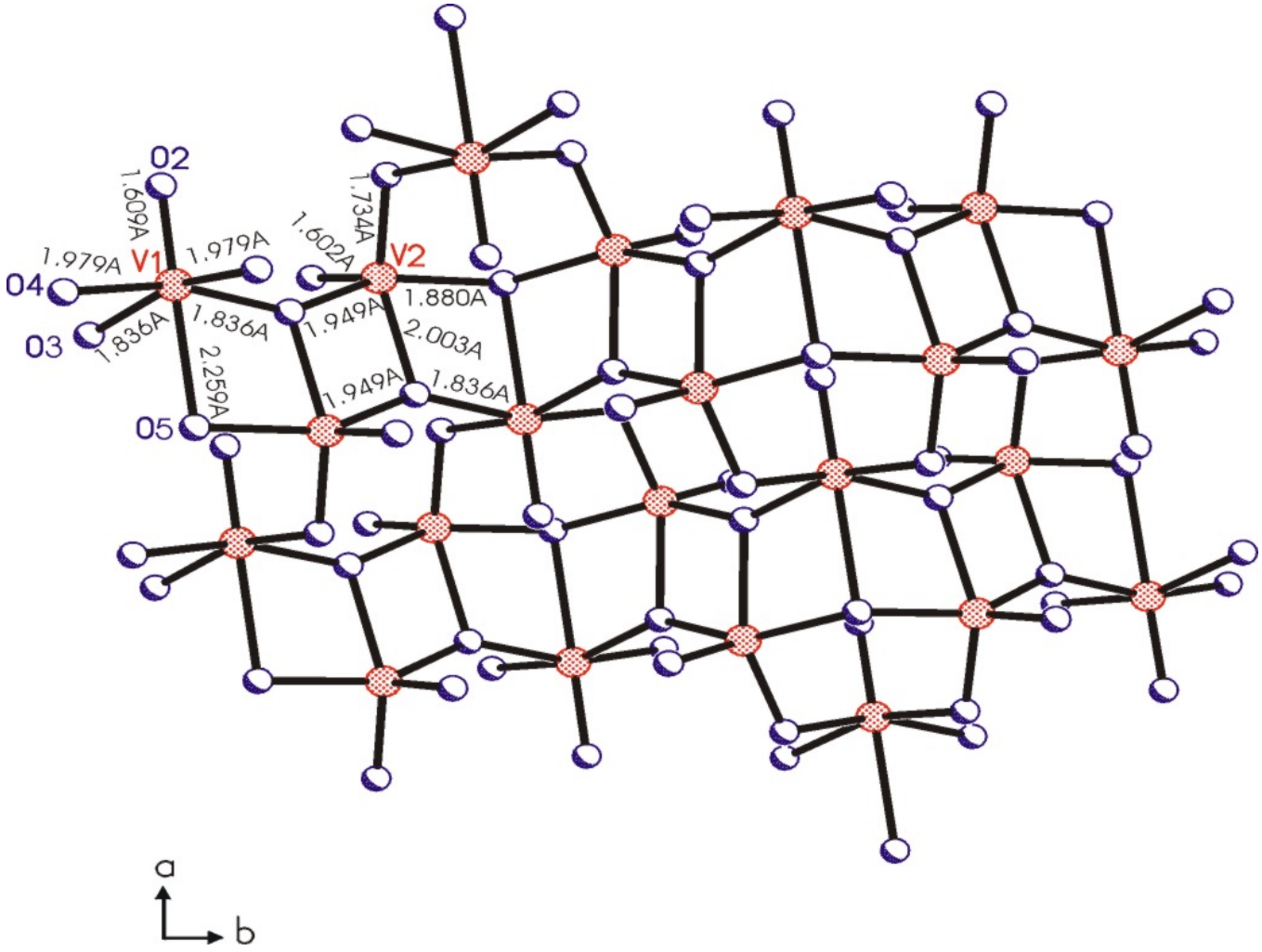

Figure 3.8 Representation of V-O bonds running along c axis in KV_3O_8 structure.

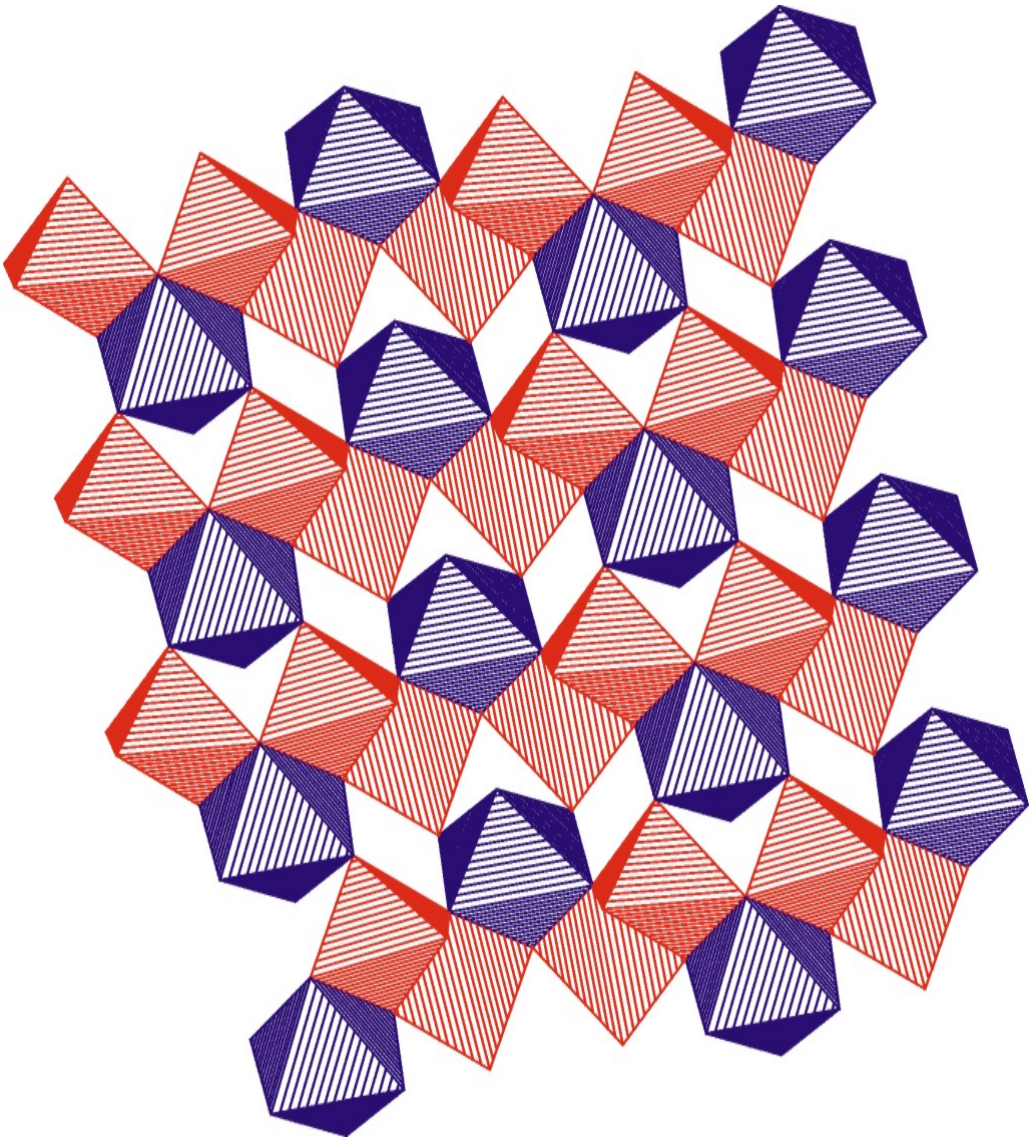

Figure 3.9 Polyhedral representations of VO_6 octahedras and VO_5 square pyramids.

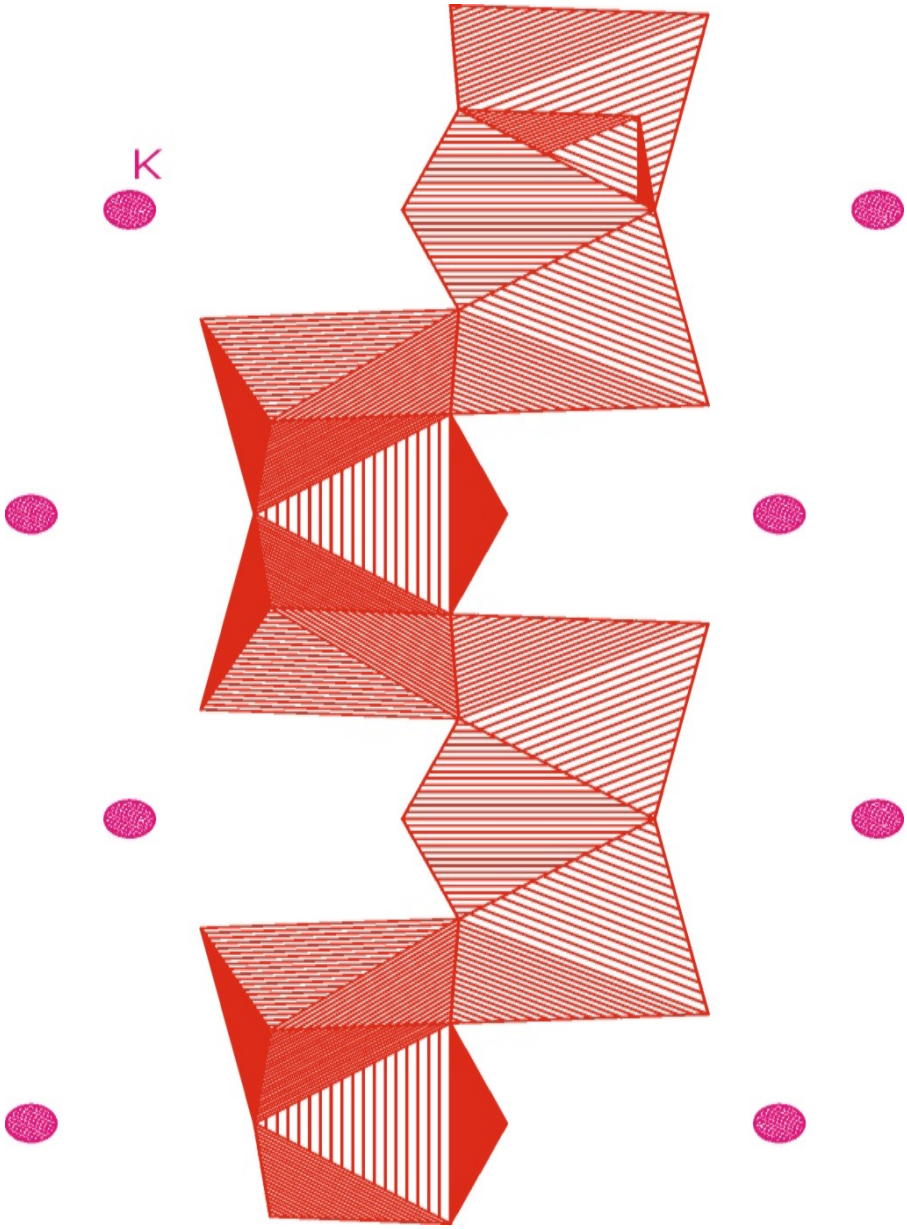

Figure 3.10 Representation of KV_3O_8 showing K atoms

CHAPTER 4

SYNTHESIS AND CHARACTERIZATION of $PbVO_3Cl$

4.1 Introduction

Water is the most important solvent in the nature. The remarkable properties of water and its solutions have been used in the synthesis of a new lead chlorovanadate.

There are many studies that have been done on oxides in the Pb-V-O systems. Vanadium oxides represent a large family of compounds which have been investigated due to their wide applications, especially in the field of catalysis. For these reasons many papers about synthesis and crystal chemistry of vanadates, vanadium bronzes, and vanadium phosphates have been published in the past [58].

In contrast, very few chlorovanadates have been synthesized to date. Considering the alkaline earth chlorovanadates, only two series of compounds are actually known. The first series with the formula $A(VO_4)_3Cl$, obtained for A= Ca, Sr, Ba, exhibits the apatite structure. Whereas the second one corresponds to the formula A_2VO_4Cl with A= Ca, Sr and exhibits the spodiosite structure [58].

There are also many vanadium oxides containing Pb, V, O elements in Pb-V-O system such as $Pb_{1.32}V_{8.35}O_{16.7}$ [59], PbV_2O_6 [60], $Pb_2V_3O_{8.5}$ [61], and β-$Pb_xV_2O_5$ bronzes (x = 0.3) [62].

Effectively, the V-O framework can accommodate many kind of cations including M= Li^+, Na^+, K^+, Ca^{2+}, Cu^{2+}, Ag^+, Cd^{2+}, Pb^{2+}… and resulting in a large range of structural forms depending on the M nature, and synthesis process. For instance, V_2O_5 is recognized to be particularly well suited for lithium insertions leading to the $Li_xV_2O_5$ system that appeared promising as positive electrode material for secondary lithium batteries [62].

In our laboratory, a novel chlorovanadate compound, $PbVO_3Cl$, was synthesized by hydrothermal synthesis method.

In the nature, there are several minerals such as kombatite, $Pb_{14}(VO_4)_2O_9Cl_4$ [63], vanadinite, $Pb_5(VO_4)_3Cl$ [64], with the same composition of elements. The pictures of these two natural minerals are shown in Fig 4.1. $Pb_{14}(VO_4)_2O_9Cl_4$ has one unique V position tetrahedrally coordinated by O atoms, and there are seven Pb positions with different coordination geometries. Four Pb atoms are coordinated by three or four O atoms and three or four Cl atoms at the vertices of flattened square antiprisms, with the central Pb cations displaced strongly toward the O ligands. Three Pb atoms are coordinated by five or six O atoms but have four of the ligands to one side of the Pb cation [63].

The structural unit of kombatite has a $[Pb_{14}(VO_4)_2O_9]^{4+}$ double sheet, and adjacent sheets are linked by Cl anions. Its structural unit consists of two sheets of the tetragonal PbO structure [63].

In the literature, there are three chlorovanadates, AVO_3Cl (A=Ba, Sr, Cd) [58], which exhibit same formula with the compound we synthesized. Two of them, $BaVO_3Cl$ and $SrVO_3Cl$, exhibit a chain structure same as title compound, whereas the third one $CdVO_3Cl$, has a layered structure built up from distorted rutile slabs interconnected through double pyramidal vanadium chains. They synthesized AVO_3Cl chlorovanadates in two steps. In first step, a mixture of V_2O_5 and ACO_3 (A=Ba, Sr, Cd) according to the composition AV_2O_6 was heated up to 973 K in platinum crucible for 6 hours to liberate CO_2. In the second step ACl_2 was added to the AV_2O_6 mixture in the 1:1 ratio. After grinding, the resulting mixture was sealed in an evacuated silica ampoule and then heated up to 753 K for 1 day and cooled at 8 K per hour down to 573 K. Finally, it was quenched down to room temperature. According to this procedure they obtained yellow crystals, but their structure determination could not be done due to the poor quality of these crystals and their small size [58].

(a)

(b)

Figure 4.1 Pictures of natural minerals (a) kombatite and (b) vanadinite.

In order to grow single crystals of AVO_3Cl compounds, LiCl was added to the oxides. First, a mixture of V_2O_5 and ACO_3 (in the molar ratio 5:3) was heated up to 973 K in air in a platinum crucible for decarbonation. Then, this resulting mixture, $A_3V_{10}O_{28}$, was added with 2 moles of LiCl and heated in a silica ampoule under the same conditions as those described for the synthesis of polycrystalline samples. And finally yellow single crystals were extracted from the so-obtained polyphasic samples [58].

In this thesis, our goal was to synthesize new metal oxide compounds. Here a new lead chlorovanadate, $PbVO_3Cl$, has been synthesized in aqueous solution, structurally characterized, and some of its properties explained. In this section we report

the synthesis and structural characterization of $PbVO_3Cl$. This compound is isostructural to $BaVO_3Cl$ and $SrVO_3Cl$ reported by Borel et al. [58].

4.2 Experimental Procedure

4.2.1 Synthesis of $PbVO_3Cl$

Single crystals of $PbVO_3Cl$ were obtained from a reaction mixture of $NaVO_3$ (460.5 mg, 3.8 mmol), $PbCl_2$ (992 mg, 3.56 mmol). This mixture was loaded into a 23-mL Teflon-lined autoclave. 1.66M of $B(OH)_3$ was added to fill ~ 40% of the total volume. The mixture was heated in an oven at 170^o C for 3 days and then cooled slowly to room temperature. Cooling must be done slowly, so crystallization occurs in the cooling part of the procedure.

When opened the resulting mixture, it was seen that it had solid products. The solid products were filtered, washed several times with distilled water and acetone, and finally dried in air at the room temperature. The needle shaped yellow crystals of $PbVO_3Cl$ and white crystals were formed in a yellow solution as reaction products. Yellow crystals were obtained with approximately 60-70% yields (Figure 4.2).

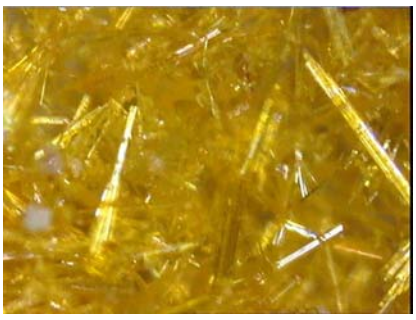

Figure 4.2 Yellow crystals of $PbVO_3Cl$ (Nikon Eclips L150 Optic Microscope, 10 X magnitudes).

$$1\ NaVO_3\ (s) \quad + \quad 1\ PbCl_2\ (s) \xrightarrow[170^oC\ for\ 3\ days]{1,66M\ B(OH)_3} PbVO_3Cl$$

Similar reactions were tried with different ratios such as: 1:3:15, 5:1:15, to increase the quality of the crystals and the yield of the reaction. All these reactions gave the same products with different yields. The best yield and better crystal quality were obtained from the reaction with 1:1:7.5 ratios.

4.2.2 X-ray Crystallographic Analyses

A single crystal of $PbVO_3Cl$ was mounted with epoxy in a capillary and was placed on a Bruker Smart 1000 CCD diffractometer under following conditions. A full reciprocal sphere corresponding to a total of 3x606 frames collected (ω-scan, 15 s per frame, 0.3^o oscillations for 3 different values of φ). Monochromatic MoKα (λ=0.71073 Å) was employed. Cell refinement and data reduction were carried out with the use of the program SAINT [43]. Face-indexed absorption corrections were made with the program XREP [44]. The structures were solved by direct methods with the program SHELXS and refined by full-matrix least squares techniques with the program SHELXL in the SHELXTL-97 [44] suite. Further crystallographic details were given in Table 4.1.

Atomic coordinates and equivalent isotropic displacement coefficients, and anisotropic displacement coefficients were given in Table 4.2 and Table 4.4, respectively. All bond distances and bond valence were given in Table 4.3. The bond angles were given in Table 4.5.

Table 4.1 Crystallographic Data for $PbVO_3Cl$.

Formula	$PbVO_3Cl$
Fw	341.62
Crystal system	Orthorhombic
Space group	Pnma
Z	3
a, Å	10.022(2)
b, Å	5.2875(11)
c, Å	7.1714(14)
$\alpha=\beta=\gamma$ deg	90
V, $(Å)^3$	380.00(13)
Dcalc, g/cm^3	4.058
μ, mm^{-1}	35.376
2θ range, deg	$3.49 – 28.88^o$

Table 4.2 Atomic Coordinates ($x10^4$) and Equivalent Isotropic Thermal Parameters of $PbVO_3Cl$.

Atom	X	Y	Z	Ueq
Pb1	0.32991	0.25000	0.61540	0.0093(3)
V1	0.47255	0.25000	0.06797	0.0054(4)
Cl1	0.39510	-0.25000	0.44701	0.0082(5)
O1	0.41086	0.00848	0.88669	0.0064(9)
O2	0.36055	0.25000	0.22921	0.0070(12)

Table 4.3 Bond Lengths (Å) and Bond Valence (italic) in $PbVO_3Cl$.

Environment of Pb(1)			Environment of V(1)		
Pb(1) - O(1)	2.464(4)	*0.386(4)*	V(1) – O(1)	1.827(5)	*0.94(1)*
Pb(1) - O(1)	2.464(4)	*0.386(4)*	V(1) – O(1)	1.827(5)	*0.94(1)*
Pb(1) - Cl(1)	2.7912(19)	*0.39(2)*	V(1) – O(1)	1.928(4)	*0.713(8)*
Pb(1) - Cl(1)	2.9794(11)	*0.232(7)*	V(1) – O(1)	1.928(4)	*0.713(8)*
Pb(1) - Cl(1)	2.9794(11)	*0.232(7)*	V(1) – O(2)	1.606(6)	*1.70(3)*
Pb(1) – Cl(1)	3.277	*0.104*			
<Pb(1) – O, Cl>	2.74		<V(1) – O>	1.82	
∑ij sij =		*1.73(2)*	∑ij sij =		*5.00(2)*

Environment of O(1)			Environment of O(2)		
O(1) – V(1)	1.928(4)	*0.713(8)*	O(2) – V(1)	1.606(6)	*1.70(3)*
O(1) – V(1)	1.827(5)	*0.94(1)*			
O(1) – Pb(1)	2.464(4)	*0.386(4)*			
<O(1) – V, Pb>	2.073(13)		<O(2) – V>	1.606(6)	
∑ij sij =		*2.04(1)*	∑ij sij =		*1.70(3)*

Environment of Cl(1)		
Cl(1) – Pb(1)	2.7912(19)	*0.39(2)*
Cl(1) – Pb(1)	2.9794(11)	*0.232(7)*
Cl(1) – Pb(1)	2.9794(11)	*0.232(7)*
Cl(1) – Pb(1)	3.277	*0.104*
< Cl(1) – Pb>	3.01(4)	
∑ij sij =		*0.96(2)*

The results refer to the equation $\sum s(M-L)= \sum \exp[(r_o-r)/0.37]$ with r_o= 1.803(3)Å, 2.112(4)Å, and 2.4395 Å for V^{5+}-O, Pb^{2+}-O, and Pb^{2+}-Cl respectively [57]. V^{5+}-O, Pb^{2+}-O distances are from the table in reference 52. Pb^{2+}-Cl distance was calculated using the formula in the same reference.

s= individual bond valences, r = bond distances in structure and r_o = empirically derived single M-L bond distance in angstrom.

Table 4.4 Anisotropic Displacement Coefficients ($Å^2 x\ 10^3$) of $PbVO_3CI$.

Atom	U11	U22	U33	U23
Pb1	0.00978	0.00893	0.00917	0.00000
V1	0.00864	0.00275	0.00475	0.00000
Cl1	0.01019	0.00597	0.00848	0.00000
O1	0.01154	0.00032	0.00727	-0.00208
O2	0.01063	0.00604	0.00426	0.00000

Table 4.5 All Bond Angles (degrees) of $PbVO_3Cl$.

O1-Pb1-O1	62.6(2)	O2-V1-O1	108.7(2) x 2
O1-Pb1-Cl1	78.61(10) x 2	O1-V1-O1	96.6(3)
O1-Pb1-Cl1	135.14(11) x 2	O2-V1-O1	105.0(2) x 2
O1-Pb1-Cl1	77.72(11) x 2	O1-V1-O1	145.29(10) x 2
Cl1-Pb1-Cl1	73.65(4) x 2	O1-V1-O1	80.27(19) x 2
Cl1-Pb1-Cl1	125.08(7)	O1-V1-O1	83.2(3)

3.2.3 Results and Discussion

The compound having a formula $PbVO_3Cl$ was prepared from the reaction of $NaVO_3$, and $PbCl_2$ in boric acid as needle shaped yellow crystals. Structure of the lead chlorovanadate, $PbVO_3Cl$, consists of a chain of VO_5 and $[PbCl]_n$ sheets running along b-axis as shown in Figure 4.3. In figure 4.3, the unit cell of $PbVO_3Cl$ is viewed down the b-axis. The edge-sharing VO_5 pyramids with a trans configuration were formed by $[VO_3]_n$ chains (Figure 4.4). Such chains have already been observed in the AV_3O_7 type of compounds [65], and also isostructural AVO_3Cl (A=Ba, Sr, Cd).

Each of the V centers has square pyramidal geometry coordinated by five O atoms. The VO_5 square pyramids of $PbVO_3Cl$ exhibit one short apical V-O bond to O2 atom of 1.606(6) Å corresponding to the free apical site, and four longer bonds with basal oxygen that ranges from 1.827(5) to 1.924(4) Å corresponding to the oxygen atoms shared between the pyramids (Figure 4.4). The VO_5 square pyramid has a distorted square pyramidal geometry with the O1-V-O2 angles ranging from 108.7(2) to 105.0(2).

$[PbCl]_n$ sheets reside between the chains of VO_5 square pyramids. Connection between VO_5 pyramids and PbCl sheets are shown in Figure 4.3. Each lead atom is coordinated by both O and Cl atoms. Lead has two equal bonds with oxygen atoms with a bond distance of 2.464(4) Å. In addition, lead has three bonds to chlorine atoms that range from 2.792(19) to 2.979(11) Å and one longer bond to fourth chlorine atom with a distance of 3.277 Å. Connections between PbCl sheets are made by long Pb-Cl bonds. In Ref. 40, Pb-O bonds range from 2.36(2) Å to 3.27(2) Å. All bonds for lead atom are in agreement with the articles reported by N. Henry [61] and by M. Cooper [63].

The relation between bond length and bond valence were studied to show formal charge on the atom in $PbVO_3Cl$ using the empirical relationship developed by Brown and Alternatt [57]. The valence of a given atom is calculated from sum of the individual bond strengths of M-L bonds. The calculated bond valence sums were given in Table 4.3. Calculations show that vanadium is pentavalent, chloro is monovalent, and lead and oxygen are divalent. These results are in agreement with the expected oxidation states. The square pyramidal vanadium has an oxidation state of +5. This assignment of oxidation state is consistent with the overall charge balance of the compound and confirmed by the valence sum calculations which gave a value of 5.00(2) for V(1).

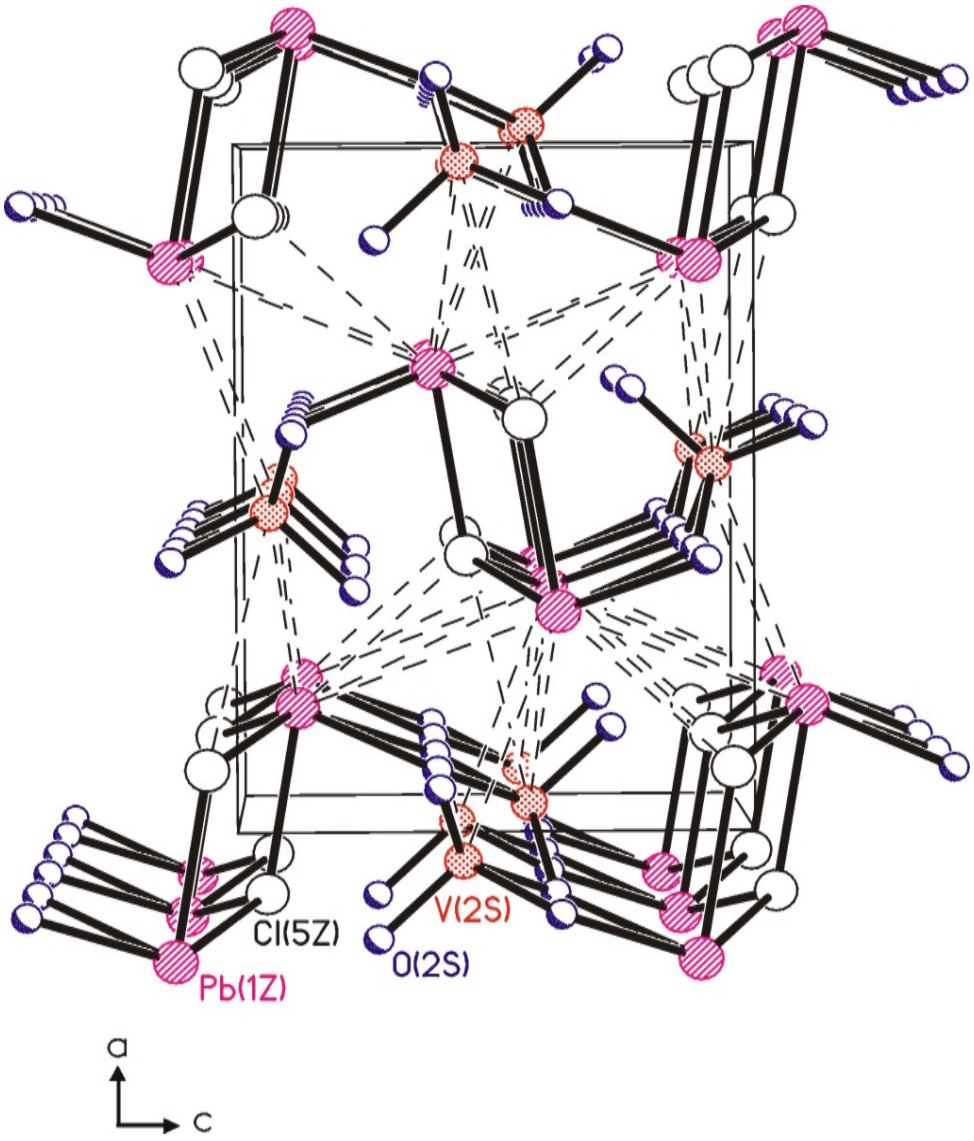

Figure 4.3 Unit cell view of $PbVO_3Cl$ running along b axis.

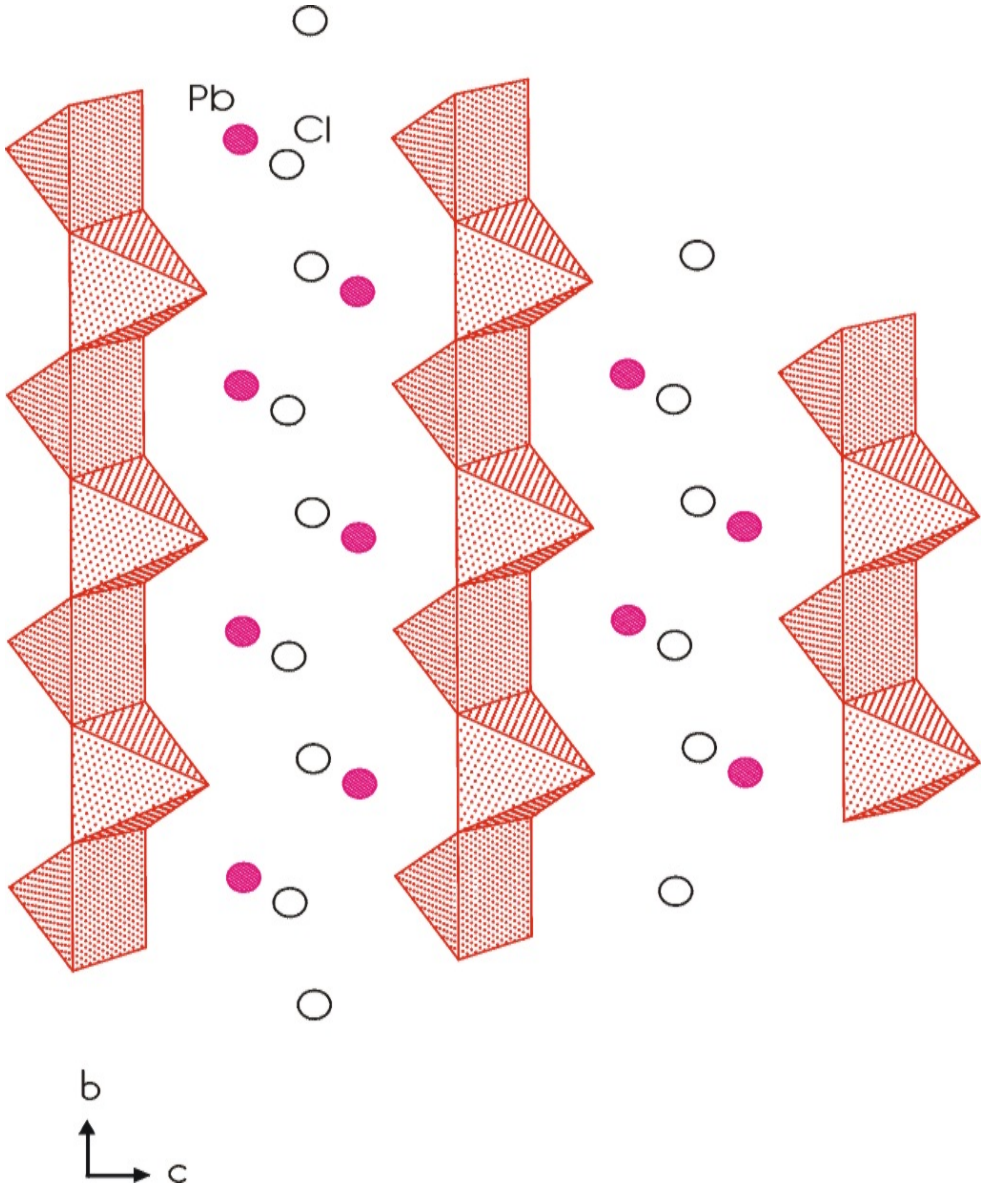

Figure 4.4 Polyhedral projection of the structure of $PbVO_3Cl$ along a axis showing the edge-sharing VO_5 pyramids with a trans configuration.

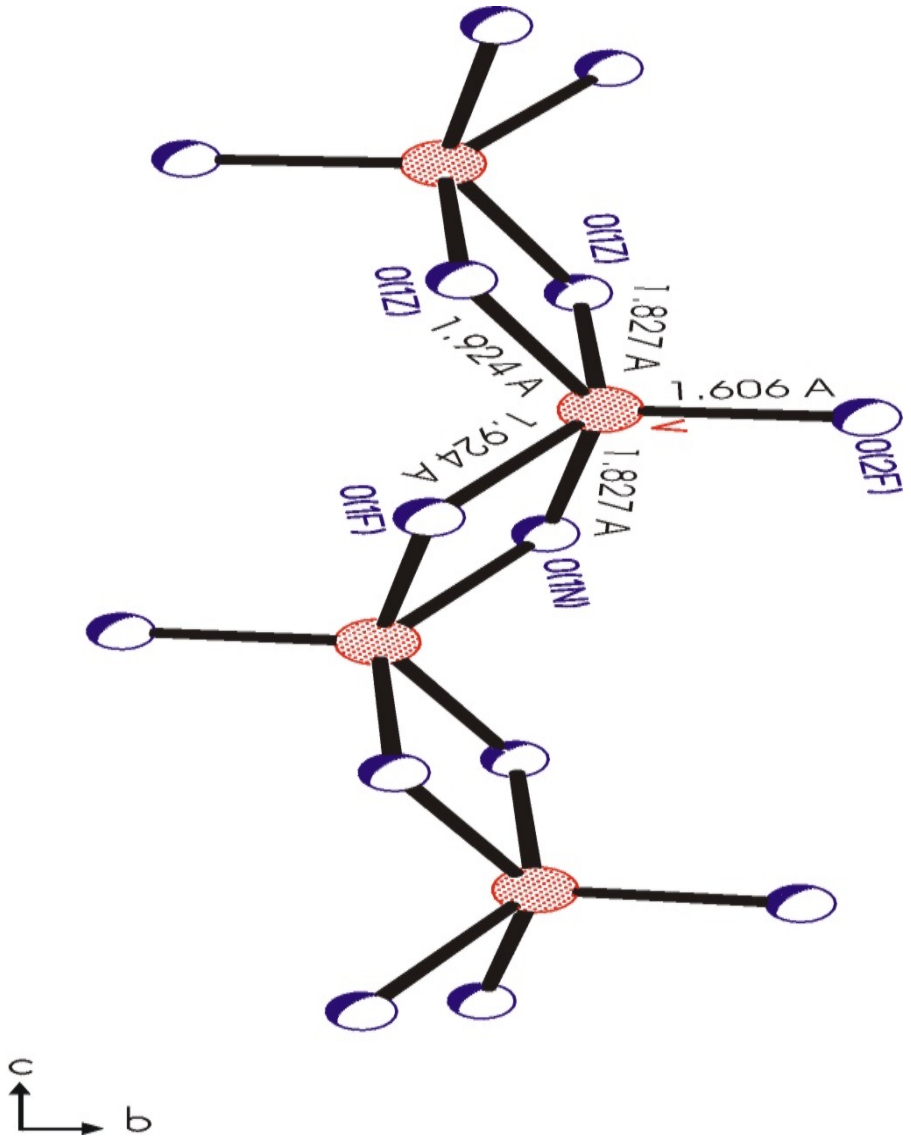

Figure 4.5 View of VO_5 bonds in $PbVO_3Cl$ structure running along a axis.

Vanadium has three oxidation states in minerals: 3+, 4+, 5+. Trivalent V has the electron configuration $3s^2 3p^6 3d^2$ and occurs mainly in octahedral coordination. In an octahedral ligand field, the two unpaired d electrons occupy the t_{2g} orbitals and are responsible for the paramagnetic and optical properties of V^{3+} compounds. Many minerals containing V^{3+} as the only transition element are green (e.g., garnet) [66].

Tetravalent vanadium has the electron configuration $3s^2 3p^6 3d^1$ and occurs in 5 or 6 coordination. In both coordination, the degenerate t_{2g} and e_g orbitals are further split and the d electron occupies one of the nonbonding orbitals ($3d_{xy}$): it is responsible for the paramagnetic and optical properties of V^{4+}. The colors of minerals containing V^{4+} are in the green/blue range, but minor contents of V^{5+} or interaction with other transition metals or OMCT bands (oxygen-metal charge transfer) can produce different colors. For example, sincosite, $Ca(VO)_2(PO_4)_2(H_2O)_5$, and simplotite, $Ca(VO)_2(VO_4)_2(H_2O)_5$, are green, minasragrite, $VOSO_4(H_2O)_5$, and pentagonite, $Ca(VO)(Si_4O_{10})(H_2O)_4$, are blue, and many mixed-valent V^{4+}/V^{5+} minerals are black or dark colored (e.g. melanovanadinite, $Ca_2V_8O_{20}(H_2O)_{10}$) [66].

Pentavalent vanadium has the electron configuration $3s^2 3p^6 3d^0$ and forms different kinds of coordination polyhedra: tetrahedral coordination which occurs also in structures with other transition elements of d^0 configuration (e.g. Ti^{4+}, Cr^{6+}, Mo^{6+}, W^{6+}), and 5 and 6 coordination. Minerals containing V^{5+} are almost always colored even though they have no d electrons. Interactions with other transition metals, minor amounts of V^{4+}, and OMCT bands cause a broad range of color from red through brown [descloizite, $ZnPb(VO_4)(OH)$] and orange [schoderite, $Al_2(PO_4)(VO_4)(H_2O)_8$] to yellow [carnotite, $K_2(UO_2)_2(V_2O_8)(H_2O)_3$] and green [fernandinite, $Ca_{0.6}(V_8O_{20})(H_2O)_{10}$] [66].

According to this, the title compound that synthesized in our lab has pentavalent vanadium and its electron configuration is $3s^2 3p^6 3d^0$.

Clark [67] defined a vanadyl bond as one which has a short bond length in the range 1.54-1.68Å. It is a multiple bond with a π-component arising from electron flow from O(pπ) to V(dπ) orbitals. In 5 and 6 coordinated (V^4+O_n) and (V^5+O_n) polyhedra, equatorial bonds occur in a cis arrangement to the vanadyl bonds, and they are longer than the vanadyl bonds. A viewed in Table 4.3, $PbVO_3Cl$ has one vanadyl bond with oxygen atom with a bond distance of 1.606(4) Å, and it can be seen this compound is in agreement with literature.

The number of vanadyl, equatorial, and trans bonds in a polyhedron may be indicated by using a multiple coordination number in which the numbers of bonds are

listed in the order vanadyl+ equatorial (+ trans). Thus, 1+4 coordination indicates 5 coordination with one vanadyl bond and four equatorial bonds, and 2+2+2 coordination indicates 6 coordination with two vanadyl bonds, two equatorial bonds, and two trans bonds [66]. In the presence of this knowledge title compound has 1+4 coordination number.

Five and six coordinated V^{5+} are characterized by the occurrence of one and two strong vanadyl bonds, respectively. Their presence in mineral and synthetic structures causes a larger variation of vanadyl, equatorial, and trans bond lengths in ($V^{5+}O_n$) polyhedra than in ($V^{4+}O_n$) polyhedra. Figure 4.6 and 4.7 show the variation of vanadyl, equatorial bond lengths in different ($V^{5+}O_n$) polyhedral geometries. There are distinct populations of V-O bond lengths, separated by ranges in which no, or only a few, bond lengths occur. This feature allow us to define different types of V^{5+}-O bonds and different ($V^{5+}O_n$) coordinations [66].

As it is seen in Figure 4.6 and 4.7, in five coordination (1+4 and 2+3), there is a minimum at 1.74-1.76Å for vanadyl bonds. In six coordination (1+4+1 and 2+2+2, there is also a minimum at 1.74-1.75 Å. Thus, we can define a vanadyl bond in five and six coordinations as a bond shorter than 1.74 Å [66].

In five coordination, the equatorial bond can be defined as a bond longer than 1.74 Å. Figure 4.6 shows the variation in length for 1+4 and 2+3 coordinations. The variation in equatorial bond length for 1+4 coordination is generally between 1.74 and 2.04 Å, with a maximal frequency at 1.88 Å (Figure 4.6a). Average bond lengths of V^{5+}-$O_{Vanadyl}$ and V^{5+}-$O_{Equatorial}$ for square pyramids have reported by Schindler as 1.59 Å and 1.89 Å, respectively [66]. As viewed in Table 4.3, bond length for $<V(1) - O_{Equatorial}>$ and $<V(1) - O_{Vanadyl}>$ are 1.877 Å, and 1.606 Å, respectively. This result is in agreement with the values reported by Schindler.

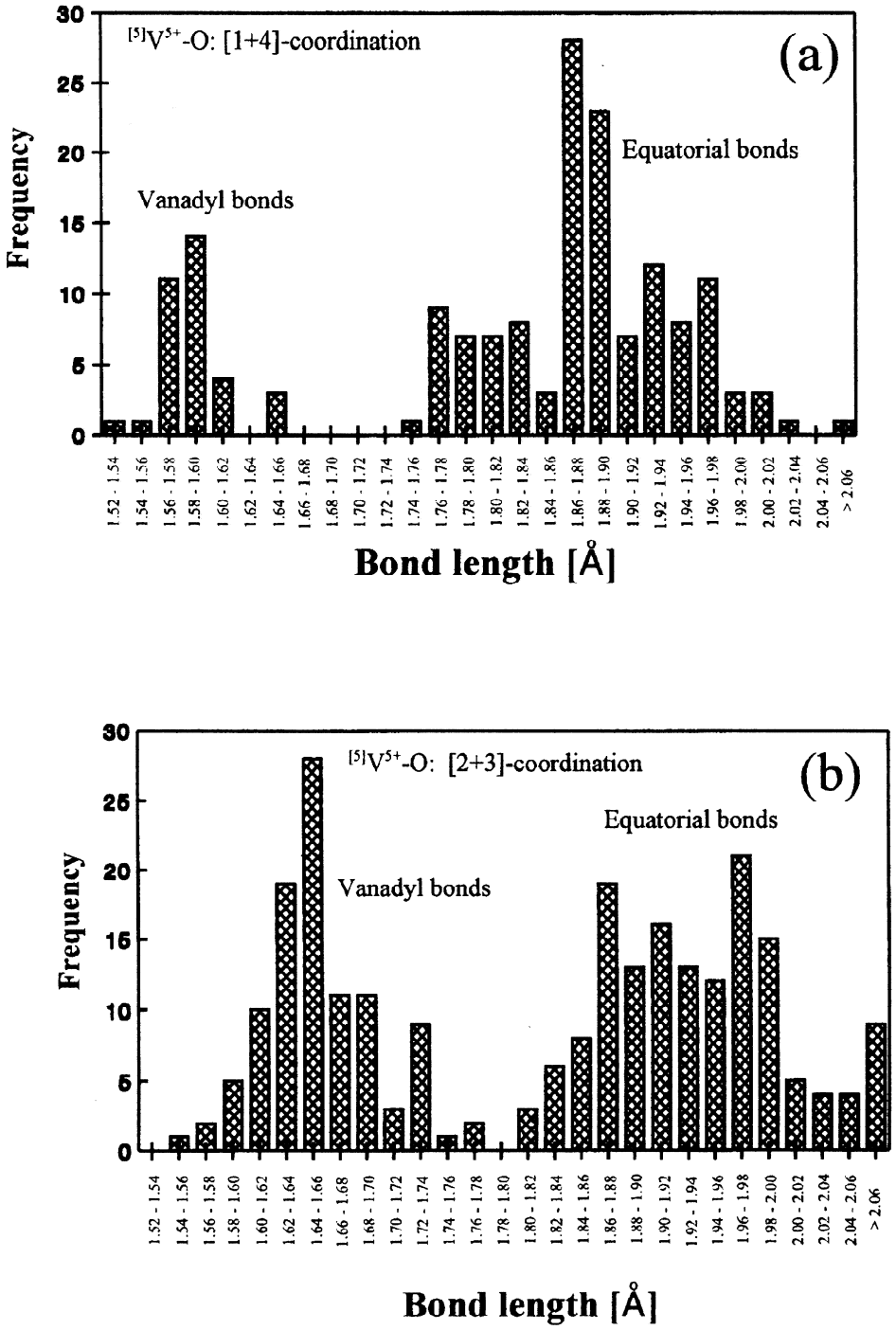

Figure 4.6 The distribution of individual bond lengths in ($V^{+5}O_5$) polyhedra in mineral and inorganic crystal structures: (a) [1+4] coordination and (b) [2+3] coordination.

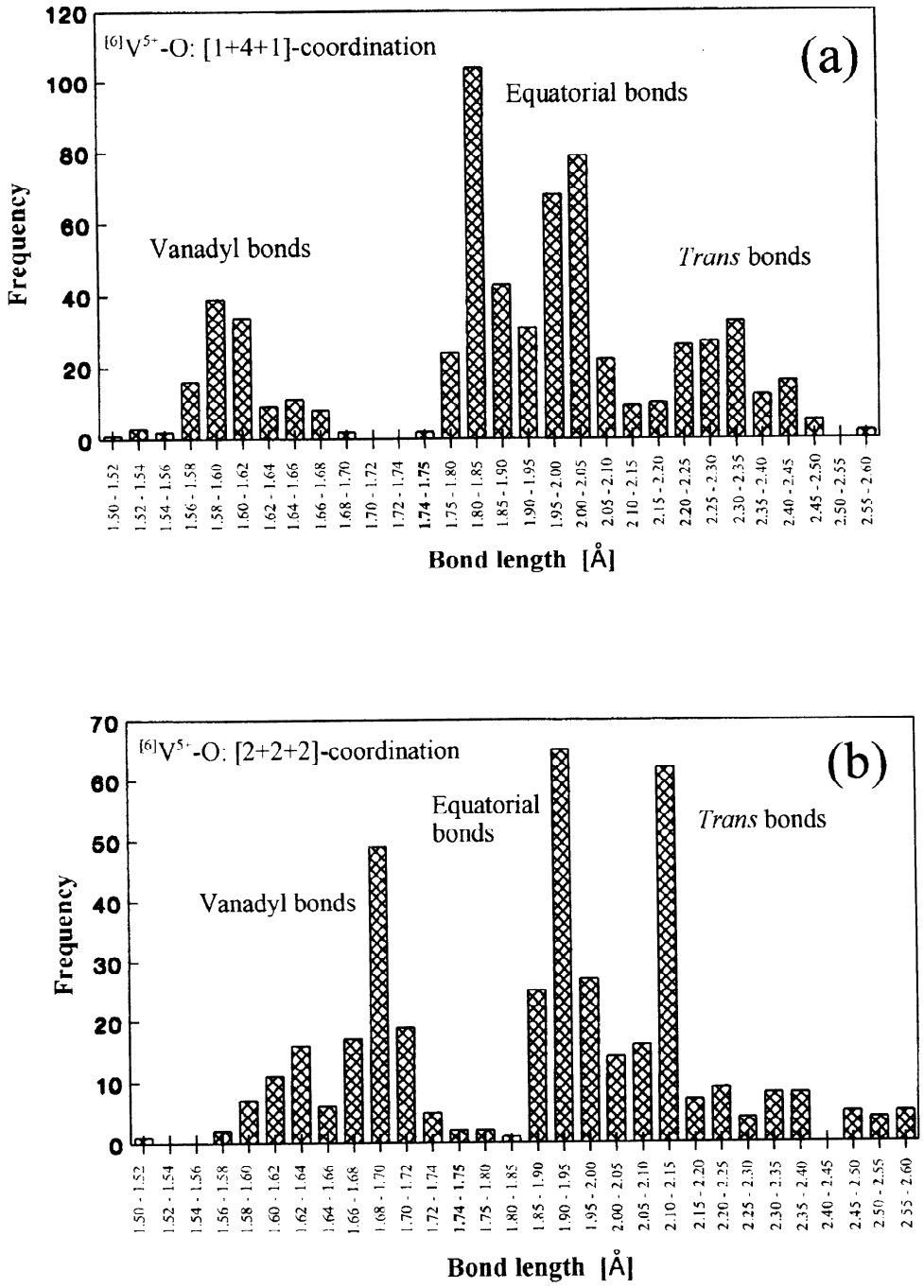

Figure 4.7 The distribution of individual vanadyl, equatorial, and trans bonds in ($V^{5+}O_6$) polyhedra in mineral and inorganic crystal structures: (a) [1+4+1] coordination and (b) [2+2+2] coordination

Examination of reported crystals with an EDX-equipped Philips XL 30S FEG SEM gave results consistent with the stated compositions. Atomic percentages of the elements of O, Cl, V, and Pb are 38.33%, 15.67%, 14.85%, and 30.60%, respectively. According to the EDX results and peaks of the yellow needle crystals were given in Table 4.6 and in Figure 4.8, respectively.

Table 4.6 EDX results of yellow needle crystals ($PbVO_3Cl$).

Element	**Weight %**	**Atomic %**
O	7.52	38.88
Cl	6.72	15.67
V	9.14	14.85
Pb	76.62	30.60
Total	100.00	100.00

$PbVO_3Cl$ was synthesized in high yield crystalline form and analyzed by powder X-ray diffraction. The resulting product had two phases that were yellow needle crystals and white crystals. White crystals were identified by powder X-ray diffraction. The X-ray diffraction pattern of white powder matched with $PbCl_2$ (Figure 4.9). X-ray powder peaks of yellow needle crystals ($PbVO_3Cl$) did not match with any compound in the XRD database (Figure 4.10).

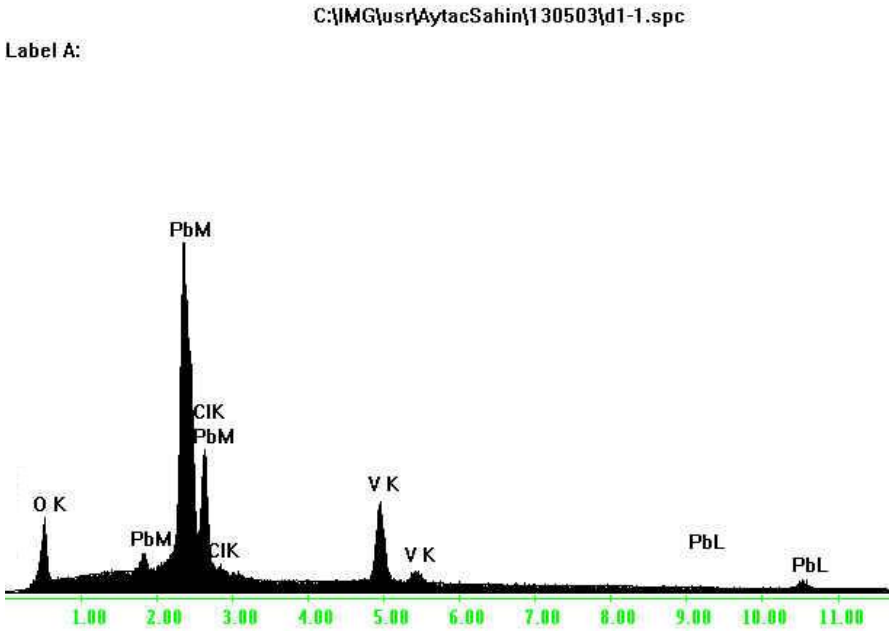

Figure 4.8 The SEM EDX peaks of $PbVO_3Cl$.

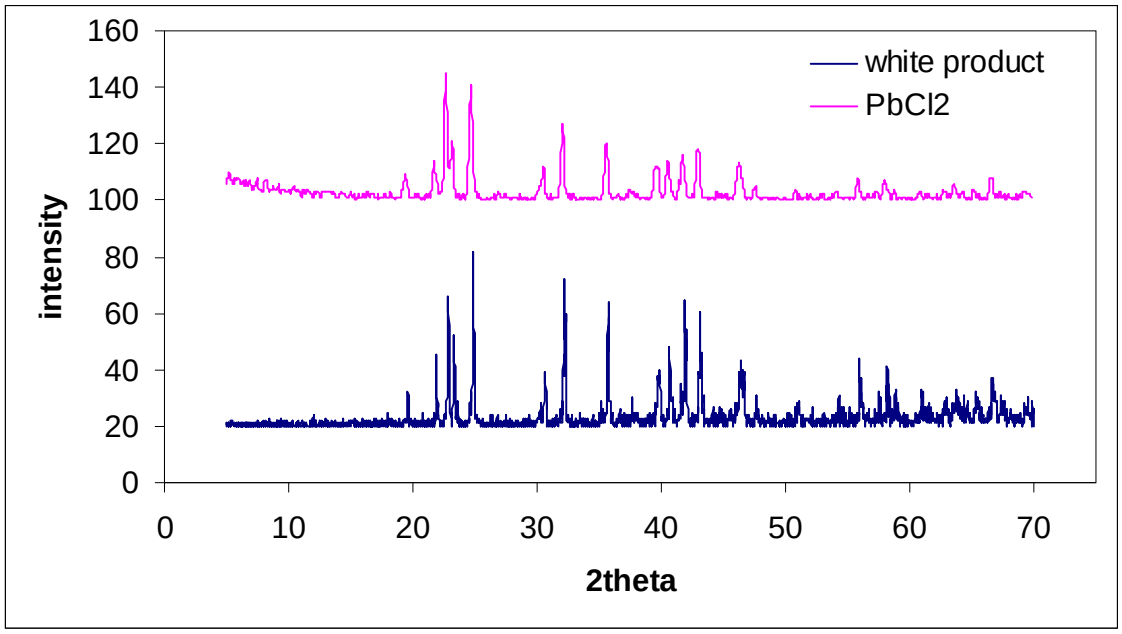

Figure 4.9 Powder patterns of $PbCl_2$ and white product.

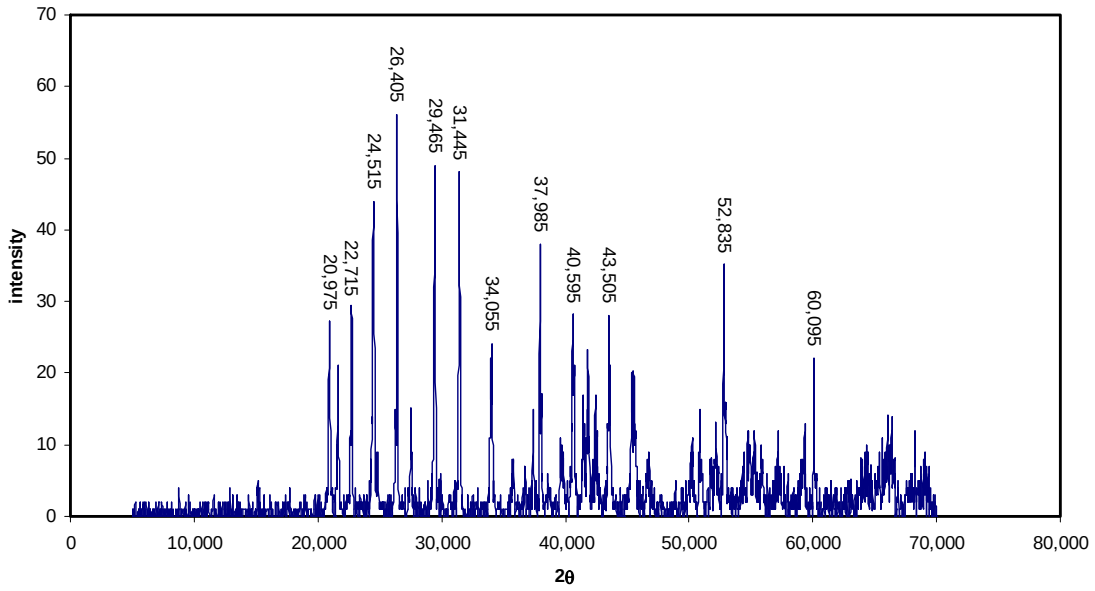

Figure 4.10 Powder pattern of $PbVO_3Cl$.

The infrared spectrum of $PbVO_3Cl$ was run on a powder sample in the form of a pellet. In an infrared spectrum, the vanadyl bond gives rise to a very strong sharp V=O stretching bond at 985 ± 50 cm^{-1} [66, 68]. The presence of a strong band at 962 cm^{-1}, which is indicative of the vanadyl V=O bond in the structure, suggests that $PbVO_3Cl$ contain this bond. Thus, this explains why one of the bonds with oxygen is double bond at approximately 1.60 Å. Infrared spectrum of $PbVO_3Cl$ is shown in Figure 4.11. Multiple features attributable to the bridging V-O-V groups are found in the 840-400 cm^{-1} region [68]. The peaks at 739 cm^{-1} and 519 cm^{-1} show the V-O-V in-plane vibration and V-O-V out-of-plane vibration, respectively [68, 69].

The TGA curve of the compound shows one major weight loss between 368^{o}C and 510^{o}C. The weight loss was 0.539mg (10.55%). Molecular weight of $PbVO_3Cl$ is 341.55g. 10.55% of this value is 34.15g. This shows that one major weight losses comes from the losses of one Cl element. The result of DSC thermal analysis shows one endothermic peak at the same range about at 480^{o}C. These two analyses are in agreement with each other and this can be attributed to the decomposition of the compound (Figure 4.12).

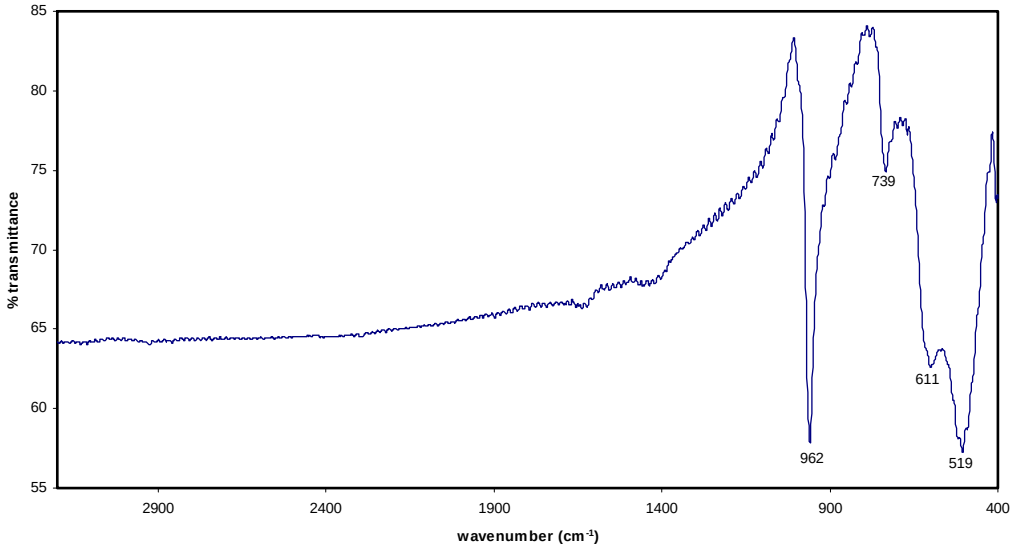

Figure 4.11 Infrared spectrum of $PbVO_3Cl$.

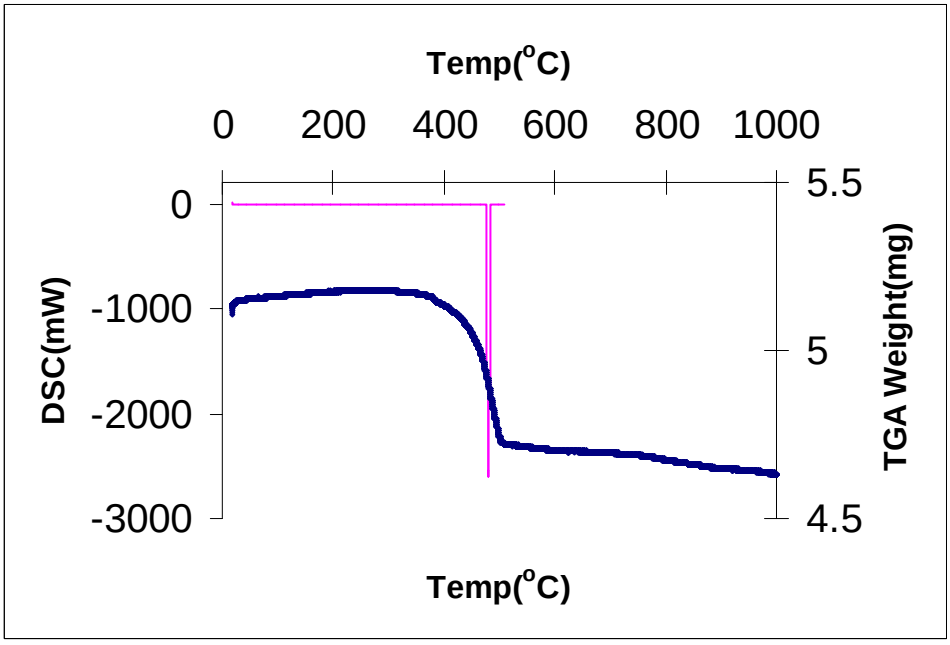

Figure 4.12 TGA and DSC curve of $PbVO_3Cl$.

CHAPTER 5

CONCLUSIONS

Hydrothermal method has been used for the all reactions and it was proven to be a good procedure for synthesizing of new metal oxide crystals.

This research has focused on synthesis and structure solution of single crystals of a novel lead chlorovanadate compound, $PbVO_3Cl$, and of a known alkali-metal trivanadate compound, KV_3O_8. Most vital part of this thesis is the structure solution of crystals that were obtained.

The needle shaped yellow crystals of $PbVO_3Cl$ compound have synthesized by hydrothermal method. This compound was prepared from the reaction of $NaVO_3$, and $PbCl_2$ in 1.66M of boric acid solution (with 1: 1: 7.5 mole ratios). These needle shaped yellow crystals were obtained at 170^o C for 3 days. The compound crystallizes in the space group Pnma of the orthorhombic system. Structure of the lead chlorovanadate, $PbVO_3Cl$, consists of a chain of VO_5 and $[PbCl]_n$ sheets running along b-axis. The edge-sharing VO_5 pyramids with a trans configuration were formed by $[VO_3]_n$ chains. Such chains have already been observed in the AV_3O_7 type of compounds [65], and this compound is isostructural to $BaVO_3Cl$ and $SrVO_3Cl$ reported by Borel et.al [58]. Each of the V centers has square pyramidal with the oxidation state of 5.00(2).

A known alkali metal trivanadate compound, KV_3O_8, have also synthesized. The compound KV_3O_8 has been prepared by hydrothermal synthesis at 170^o C for 3 days from KVO_3, and $PbCl_2$ in 1.66M of $B(OH)_3$ solution. This compound originally synthesized by through very complicated reaction process. We were able to obtain these crystals very easily after trying a number of different reaction conditions. At the end this compound was able to be obtained with only using KVO_3 in $B(OH)_3$ solution in 2 days.

The crystal structure was determined by single crystal X-ray diffraction and found to crystallize in monoclinic crystal system with space group P2(1)/m. The orange hexagonal plate-shaped crystal, KV_3O_8, is composed of a layered structure with V_3O_8 layers consisting of VO_6 octahedra and VO_5 square pyramids. The compound has two unique vanadium atoms (V1, V2) with different coordination environment. The V1 has

a distorted octahedral environment and the V2 has a square pyramidal coordination environment. All V are pentavalent with approximately the oxidation state of +5.

Water has proven to be excellent medium to synthesize novel compounds under the hydrothermal conditions.

After all the experiments, one new and one known compound were able to be obtained and analyzed their some properties. By slightly varying the reaction conditions, good single crystals were able to be prepared.

In the future work, we should try to change V with other transition metals.

REFERENCES

[1] A. Rabenau, "The Role Hydrothermal Synthesis in Preparative Chemistry", *Angew. Chem*., *Int. Eng. Ed.*, **24**, 1985, 1026-1040.

[2] R.A. Laudise, The Growth of Single Crystals, (Prentice-Hall, Englewood Cliffs, NJ, 1970).

[3] A.N. Lobachev, Crystallization Processes under Hydrothermal Conditions, (Consultants Bureau, New York, 1973).

[4] R. Roy, "Acceleration the Kinetics of Low-Temperature Inorganic Syntheses", *J. Solid State Chem*., **111**, 1994, 11-17.

[5] K. Byrappa, Hydrothermal Growth of Crystals, (Pergamon Press, Oxford, UK, 1992).

[6] M. Yoshimura, and H. Suda, Hydrothermal Processing of Hydroxyapatite": Past, Present, and Future, in: "Hydroxyapatite and Related Materials (P. W. Brown and B. Constanz, eds., CRC Press, 1994, 45-72).

[7] K. Byrappa, and M. Yoshimura, Handbook of Hydrothermal Technology, A Technology for Crystal Growth and Material Processing, (Noyes, New Jersey, 2001).

[8] Sir Roderick Murchison (1840s), (cited by S. Somiya).

[9] H.L. Barnes, Geochemistry of Hydrothermal Ore Deposits", (Wiley Interscience Publication, New York, 1979).

[10] K.F.E. Schafhault, *Gelehtre Anzeigen Bayer. Akad.*, **20**, 1845, 557, 569, 575, 592.

[11] R.W. Shaw, T.B. Brill, A.A. Clifford, C.A. Eckert, E.U. Franck, *Chem. Eng. News*, **26**, 1991, Dec.23.

[12] R. Bunsen, *Ann.*, **65**, 1848, 70.

[13] H. deSenarmont, *Ann.Chem. Phys.*, **32**, 1851, 129.

[14] R. Roy, and O.F. Tuttle, "Investigations under hydrothermal conditions", *Physics and Chemistry of the Earth*, vol. 1, L.H. Ahrens, K. Rankama, and S. K. Runcorn (Eds.), (Pergamon, New York, 1956, 138).

[15] G.W. Morey, *J. Am. Ceram. Soc*., **36**, 1953, 279.

[16] P.W. Bridgeman, The Physics of High Pressure, (Bell. London, 1949).

[17] R.A. Laudise, and A.A. Ballman, in Kirk-Othmer Encyclopedia of Chemical Technology, (2nd Ed. John Wiley and Sons, New York, **18**, 1969, 105).

[18] P.G. Jessop, L. Walter, Chemical Synthesis Using Supercritical Fluids", (Wiley VCH: Weinheim, 1999).

[19] R.W. Goranson, "Solubility of Water in Granite Magmas", *Amer. J. Sci.,* **22**, 1931, 481-502.

[20] R. Nacken, Artificial Quartz Crystals, etc., U.S. *Office of Technical Services Report,* PB-18-748 and 28-897 (1946).

[21] R.M. Barrer, "Syntheses and Reactions of Mordenite", *J. Chem. Soc*., 1948, 2158.

[22] A.R. West, Solid State Chemistry and its Applications, (John Wiley and Sons, New York, 1984).

[23] U. Schubert, N. Hüsing, "Synthesis of Inorganic Materials", **5**, 2000, 181-184.

[24] M.G. Kanatzidis, "Molten alkali-metal polychalcogenides as reagents and solvents for the synthesis of new chalcogenide materials", *Chem. Mater*., **2**, 1990, 353.

[25] M. Eanes, Synthesis and Characterization of Alkali Silver Chalcogenides and Alkali Rare Earth Germanates by Supercritical Fluids, *Doctor of Philosophy,* (Clemson University, Dec. 2000).

[26] S.D. Haman, "Properties of electrolyte solutions at high pressures and temperatures", *Physics and Chemistry of the Earth*, **13/14**, 1981, 89.

[27] A. Laudise, *Chem. Eng. News*, **30**, 1987, Sept.28.

[28] A.T. Chien, Hydrothermal Epitaxy of Peroksite Thin Films, Doctor of Philosophy, (University of California, July 1998).

[29] R.J. Baughman, "Quartz Crystal Growth", *J. Crystal. Growth*, **112**, 1991, 753.

[30] A.A. Ballman, and R.A. Laudise, in The Art and Science of Growing Crystals, (Wiley, New York, 1963).

[31] R.M. Barrer, Hydrothermal Chemistry of Zeolites, (Academic Press, London, 1982).

[32] J. Bierlein, and T. Geir, U.S. Patent 3,949,323, April, 1976.

[33] K. Reis, A. Ramanan, and M. Whittingham, *Chem. Mater*., **2**, 1990, 219**.**

[34] Q. Chen, Y. Qian, Z. Chen, K. Tang, G. Zhou, and Y. Zhang, "Preparation of a Tl-based superconductor by a hydrothermal method", *Physica C*, **224**, 1994, 228.

[35] M. Sugita, M. Tsuji, and M. Abe, *Bull. Chem. Soc. Jpn.*, **63**, 1990, 1978.

[36] X. Zhao, R. Roy, K. Cherian, and A. Badzian, *Science*, **385**, 1997, 513.

[37] M. Hosaka, in Progress in Crystal Growth and Characterization, (Pergamon Press, London, 1991).

[38] M. Whittingham, J.D. Guo, R. Chen, T. Chirayil, G. Janauer, and P. Aavalij, "The hydrothermal synthesis of new oxide materials", *Solid State Ionics*, **75**, 1995, 257.

[39] C.N.R. Rao, "Chemical Synthesis of Solid Inorganic Materials", *Material Sciences and Engineering*, **B18**, 1993, 1-21.

[40] W.J. Dawson, and M.K. Han, Development and scale-up of hydrothermal processes for synthesis of high performance materials", In Hydrometallurgy fundamentals, technology and innovations, (Ed. J.B. Hiskey and G.W. Warren, SME Inc., 1993, 593-610).

[41] Parr Instrument Company, 211 53rd Street, Moline, Illinois 61265.

[42] J. Tanaka, and S.L. Suib, Experimental Methods in Inorganic Chemistry, (Practice Hall, New Jersey, 1999).

[43] Bruker SMART Version 5.054 Data Collection and SAINT-Plus Version 6.2.2 Data Processing Software for the SMART system, Bruker Analytical X-Ray Instruments; Inc.; Madison; WI; USA; 2000.

[44] Sheldrick G.M., SHELXTL Dos / Windows / NT Version 6.12, Bruker Analytical X-Ray instruments; Inc.; Madison; WI; USA; 2000.

[45] A.K. Brisdon, Inorganic Spectroscopic Methods, (Oxford University Press Inc., New York, 1998).

[46] Y. Idota, European patent No. 0567149 A1, 1993.

[47] M. Whittingham, R. Chen, T. Chirayil, and P. Zavalij, E*lectrochem Soc Proc.,* **96**, 1996, 76.

[48] F. Abraham, J. Boivin, G. Mairesse, and G. Nowogrocki, "The bimevox series: A new family of high performances oxide ion conductors", *Solid State Ionics"*, **40**, 1993, 934.

[49] K. Bahranowski, G. Bueno, V. Corberan, F. Kooli, E. Sewicka, R. Valenzuela, and K. Wcislo, "Oxidative dehydrogenation of propane over calcined vanadate-exchanged Mg,Al-layered double hydroxides", *Applied Catalysis A: General*, **185**, 1999, 65.

[50] M. Baerns, R. Schlogl, and B. Delmon, "Oxidative dehydrogenation of *n*-pentane on magnesium vanadate catalysts", *Catalysis Today*, **32**, 1996, 229.

[51] P.J. Hagrman, R.C. Finn, and J. Zubieta, "Molecular Manipulation of Solid State Structure: Influences of Organic Components on Vanadium Oxide Architectures", *Solid State Sciences*, **3**, 2001, 745-774.

[52] A. Muller, H. Reuter, and S. Dillinger, "Supramolecular Inorganic Chemistry: Small Guests in Small and Large Hosts", *Angew. Chem. Int. Ed.Engl.*; **34**, 1995, 2328.

[53] V.W. Day, M.F. Fredrich, W.G. Klemperer, and W. Shum, "Synthesis and characterization of the dimolybdate ion, Mo_2O_{72}"; *J. Am. Chem. Soc*.; **99**, 1977, 6146.

[54] J. Fuchs, S. Mahjour, and J. Pickardt, "Structure of the True Metavanadate Ion", *J. Angew. Chem., Int. Ed. Engl.*, **15**, 1976, 374.

[55] Jr. H.T. Evans, "The Molecular Structure of the Isopoly Complex Ion, Decavanadate ($V_{10}O_{28}^{6-}$)", *Inorg. Chem*., **5**, 1966, 967.

[56] Y. Oka, T. Yao, and N. Yamamato, "Hydrothermal Synthesis and Structure Refinements of Alkali-Metal Trivanadates AV_3O_8 (A=K, Rb, Cs)", *Mater. Res. Bull.*, **32**, 1997, 1201-1209.

[57] I.D. Brown, and D. Alternatt, "Bond-valence Parameters Obtained from a Systematic Analysis of the Inorganic Crystal Structure Database", *Acta Cryst.,* **B41**, 1985, 244-247.

[58] M.M. Borel, J. Chardon, A. Leclaire, and B. Raveau, "Chlorovandates with Original Chain and Layered Structures: AVO_3Cl (A=Ba, Sr, Cd)", *J. Solid State Chem.*, **145**, 1999, 634-638.

[59] O. Mentre, and F. Abraham, "New mixed valence compounds in the Pb-V-O system: Synthesis and crystal structure of hollandite-related $Pb_{1.32}V_{8.35}O_{16.7}$ and R-type hexagonal ferrite PbV_6O_{11}", *J. Solid State Chem.,* **125**, 1996, 91-101.

[60] G. Calestani, G.D. Andreetti, and A. Montenero, "Structure of metastable lead metavandates: the monoclinic PbV_2O_6 (II) modification", *Acta. Cryst.,* **41**, 1985, 177-179.

[61] N. Henry, O. Mentre, and F. Abraham, "$Pb_2V^{III}O(VO_4)(V_2O_7)_{0.5}$, a novel lead vanadium III vanadate possessing trivalent vanadium rutile-like chains: Relationships with related compounds", *J. Solid State Chem.,* **163**, 2002, 519-526.

[62] O. Mentre, M. Huve, and A. Abraham, "Bidimentional cationic ordering and thermal dependence in β-$Pb_xV_2O_5$ bronzes", *J. Solid State Chem.*, **145**, 1999, 186-196.

[63] M. Cooper, and F.C. Hawthorne, "The crystal structure of kombatite, $Pb_{14}(VO_4)_2O_9Cl_4$, a complex heteropolyhedral sheet mineral", *American Minerologist,* **79**, 1994, 550-554.

[64] Y. Dai, and J.M. Hughes, "Crystal Structure Refinements of Vanadinite and Pyromorphite", *Canadian Mineralogist*, **27**, 1989, 189-192.

[65] G. Liu, and J.E. Greedan, "Crystal Structures and Magnetic Properties of MV_3O_7 (M = Cd, Ca, Sr) with Square Pyramidal V(IV)", *J. Solid State Chem.*, **103**, 1993, 139.

[66] M. Schindler, F.C. Hawthorne, and W.H. Baur, "Crystal Chemical Aspects of Vanadium: Polyhedral Geometries, Characteristic Bond Valences, and Polymerization of (VO_n) Polyhedra", *Chem. Mater.*, **12**, 2000, 1248-1259.

[67] R.J.H. Clark, The Chemistry of Titanium and Vanadium, (Elsevier, New York, 1968).

[68] M.I. Khan, "Novel Extended Solid Composed of Transition Metal Oxide Clusters", *J. Solid State Chem.*, **152**, 2000, 105-112.

[69] K. Yakamoto, Infrared and Raman Spectra of Inorganic and Coordination Compounds, (4^{th} Edition, John Wiley & Sons Inc., Canada, 1986).